(2)

NAVAL POSTGRADUATE SCHOOL

AD-A246 880 Monterey, California

THESIS

SATELLITE ANOMALIES AND
ELECTROSTATIC SURFACE DISCHARGES

by

Yan Chun Wong

September, 1991

Thesis Advisor: Dr. Richard C. Olsen

Approved for public release; distribution unlimited

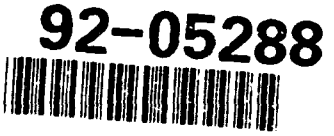

REPORT DOCUMENTATION PAGE

Form Approved OMB No. 0704-0188

1a. REPORT SECURITY CLASSIFICATION Unclassified	1b. RESTRICTIVE MARKINGS
2a. SECURITY CLASSIFICATION AUTHORITY	3. DISTRIBUTION/AVAILABILITY OF REPORT Approved to public release; distribution is unlimited
2b. DECLASSIFICATION/DOWNGRADING SCHEDULE	
4. PERFORMING ORGANIZATION REPORT NUMBER(S)	5. MONITORING ORGANIZATION REPORT NUMBER(S)
6a. NAME OF PERFORMING ORGANIZATION Naval Postgraduate School 6b. OFFICE SYMBOL (If applicable) Code 39	7a. NAME OF MONITORING ORGANIZATION Naval Postgraduate School
6c. ADDRESS (City, State, and ZIP Code) Monterey, CA 93943-5000	7b. ADDRESS (City, State, and ZIP Code) Monterey, CA 93943-5000
8a. NAME OF FUNDING/SPONSORING ORGANIZATION 8b. OFFICE SYMBOL (If applicable)	9. PROCUREMENT INSTRUMENT IDENTIFICATION NUMBER
8c. ADDRESS (City, State, and ZIP Code)	10. SOURCE OF FUNDING NUMBERS PROGRAM ELEMENT NO. / PROJECT NO. / TASK NO / WORK UNIT ACCESSION NO.

11. TITLE (Include Security Classification)
SATELLITE ANOMALIES AND ELECTROSTATIC SURFACE DISCHARGES

12. PERSONAL AUTHOR(S)
Wong, Yan C.

13a. TYPE OF REPORT	13b. TIME COVERED	14. DATE OF REPORT (Year, Month, Day)	15. PAGE COUNT
Master's Thesis	FROM _____ TO _____	1991 September	84

16. SUPPLEMENTARY NOTATION The views expressed in this thesis are those of the author and do not reflect the official policy or position of the Department of Defense or the U.S. Government.

17. COSATI CODES		
FIELD	GROUP	SUB-GROUP

18. SUBJECT TERMS (Continue on reverse if necessary and identify by block number)
Spacecraft Charging, Surface Charging
Spacecraft Anomalies, Active Charge Control

19. ABSTRACT (Continue on reverse if necessary and identify by block number)

Various aspects of the space environment can cause on-orbit satellite anomalies. Studies have shown that adverse interactions between the natural space environment and space systems can have deleterious consequences comparable to those caused by human or design errors. Electrostatic surface discharge (ESD), electron caused electromagnetic pulse (ECEMP), and single event upset (SEU) are the three most common anomaly producing mechanisms in space systems. The plasma environment, such as in geosynchronous orbit, can cause differential charging of satellite components and lead to ESD's on satellite surfaces.

By using the Spacecraft Anomaly Manager (SAM) software package, spacecraft anomaly data of operational satellites contained in the database of National Geophysical Data Center (NGDC) were analyzed. The analysis concluded that ESD is directly related to geomagnetic storm activity and ESD related anomalies are local time and seasonal dependent. Proper engineering solutions should be integrated into satellite designs to prevent ESD from causing anomalies. This can be done effectively on multi-satellite programs such as

20. DISTRIBUTION/AVAILABILITY OF ABSTRACT	21. ABSTRACT SECURITY CLASSIFICATION
☒ UNCLASSIFIED/UNLIMITED ☐ SAME AS RPT. ☐ DTIC USERS	Unclassified
22a. NAME OF RESPONSIBLE INDIVIDUAL R. C. OLSEN	22b. TELEPHONE (Include Area Code) (408) 646-2019 22c. OFFICE SYMBOL PH/OS

DD Form 1473, JUN 86 Previous editions are obsolete. SECURITY CLASSIFICATION OF THIS PAGE

Item 19 CONT'D

GPS. Active charge control is recommended for DoD satellites which cannot tolerate functional anomalies due to ESD's, and on the first flight of new satellite designs. Passive engineering solutions should be integrated into satellite designs.

Approved for public release; distribution is unlimited.

Satellite Anomalies and
Electrostatic Surface Discharges

by

Yan Chun Wong
Major, United States Marine Corps
B.S., University of Arizona, 1978

Submitted in partial fulfillment
of the requirements for the degree of

MASTER OF SCIENCE IN SYSTEMS TECHNOLOGY
(SPACE SYSTEMS OPERATIONS)

from the

NAVAL POSTGRADUATE SCHOOL
September 1991

Author: Yan Chun Wong
Yan Chun Wong

Approved by: Richard C Olsen
Richard C. Olsen, Thesis Advisor

Otto Heinz
Otto Heinz, Second Reader

R Panholzer
Rudolf Panholzer, Chairman, Space Systems Academic Group

ABSTRACT

Various aspects of the space environment can cause on-orbit satellite anomalies. Studies have shown that adverse interactions between the natural space environment and space systems can have deleterious consequences comparable to those caused by human or design errors. Electrostatic surface discharge (ESD), electron caused electromagnetic pulse (ECEMP), and single event upset (SEU) are the three most common anomaly producing mechanisms in space systems. The plasma environment, such as in geosynchronous orbit, can cause differential charging of satellite components and lead to ESD's on satellite surfaces.

By using the Spacecraft Anomaly Manager (SAM) software package, spacecraft anomaly data of operational satellites contained in the database of National Geophysical Data Center (NGDC) were analyzed. The analysis concluded that ESD is directly related to geomagnetic storm activity and ESD related anomalies are local time and seasonal dependent. Proper engineering solutions should be integrated into satellite designs to prevent ESD from causing anomalies. This can be done effectively on multi-satellite programs such as GPS. Active charge control is recommended for DoD satellites which cannot tolerate functional anomalies due to ESD's, and on the first flight of new satellite designs. Passive engineering solutions should be integrated into satellite designs.

TABLE OF CONTENTS

ACKNOWLEDGMENTS

The author wishes to express his appreciation to Professor R.C. Olsen for his scholarly advice, time, and patience. The author also wishes to thank D.J. Gorney and H.C. Koons of Aerospace Corporation for the DSCS-1 anomaly information, Captain Mike Scardera of 2nd Space Control Squadron, 2nd Space Wing Operations, USAF, for the recent GPS anomaly data, and D.C. Wilkinson and J.H. Allen of National Geophysical Data Center for the Spacecraft Anomaly Manager (SAM) software and the associated anomaly data.

I. SPACE ENVIRONMENT AND SPACECRAFT CHARGING

A. INTRODUCTION

Recent technological advances have allowed man to expand beyond the near earth environment into a new frontier. This expansion is accomplished through the launching of satellites into various earth orbits. The more satellites we launch, the more we learn about our space environment surrounding Earth. Unfortunately, the space environment has proven to be hostile to satellites and has resulted in large amounts of research being directed to determine both the causes and remedies for these hostilities. One of the areas receiving attention is in unexpected satellite anomalies.

Satellites operating in this hostile environment interact with elements such as cosmic rays, energetic protons, and plasma. Studies have confirmed that adverse interaction can cause on-orbit anomalies and can lead to serious consequences to the operation of the satellite. For instance, spacecraft charging, an anomaly producing process, has been an ongoing concern since the early days of satellite flights (Whipple, 1965). The majority of observed charging events have come from satellites in geosynchronous orbit, as first reported by DeForest (1977). The observations from Applications Technology Satellite 5 (ATS-5) showed that ATS-5 charged to potentials as high as -10,000 Volts in eclipse and -200 Volts in sunlight. Potentials of these

magnitudes can produce damaging electrostatic discharges and possibly lead to environment related anomalies.

By studying space environment related anomalies, one can determine the cause of these anomalies and then solve the charging problem through improved engineering designs. Solutions can utilize either active or passive charge control on board the spacecraft. A simple passive charge control measure such as properly grounding loose wires or increasing the shielding thickness is sometimes sufficient to solve the environmental charging problem. Active charge control may be needed if passive measures fail to resolve the problem. The magnitude of the anomaly and its economic impact must be carefully weighed to determine which control measure should be implemented. Therefore, by carefully analyzing anomaly data of various satellites, it can be determined if there is a need for active charge control aboard future Department of Defense (DoD) satellites, or if passive techniques can be relied upon. The focus of this thesis is to evaluate satellite anomalies caused by surface charging, and to determine if active charge control is necessary.

The remainder of this chapter shall briefly examine the physical processes of spacecraft charging, discharging, and their related satellite anomalies.

B. ENVIRONMENTAL INTERACTIONS

Various factors of our near earth space environment interact with spacecraft. The following is a list of environmental factors which can interact with spacecraft:

- Acoustic Noise

- Air Pressure
- Asteroids
- Atmospheric Noise
- Cosmic Rays
- Deep Space Ions
- Eclipses
- Electromagnetic Interference
- Magnetic Storms
- Micrometeors
- Plasma
- Radiation Belt
- Solar Flares

From the above list, cosmic rays, eclipses, plasma, radiation belt, and solar flares represent the environmental factors most closely related to spacecraft charging.

Spacecraft charging is the process through which a spacecraft gains an electrical potential relative to its surroundings. This accumulation of charge on a spacecraft results from interactions between spacecraft and the ambient plasma or radiation environment. Spacecraft charging can be divided into three types: 1. surface (or external) charging, 2. bulk (or internal) charging of dielectrics, and 3. passage of single high energy particles through the spacecraft. The consequences of these processes are: surface charging results in electrostatic surface discharge (ESD);

internal charging results in Electron Caused ElectroMagnetic Pulse (ECEMP); and the passage of single high energy particles usually results in Single Event Upset (SEU).

1. Surface Charging

Surface charging is by far the best known and most easily identifiable phenomenon associated with spacecraft environment interactions. It is the result of emission and collection of charged particles both to and from the exposed external surfaces of the spacecraft. Surface charging is produced by interactions between the satellite surfaces and the space plasma, magnetic field, and solar radiation (Whipple, 1965). (see Figure 1) The majority of the particles affecting the charge state are electrons and ions, with energies ranging from 1 electron volt (eV) up to 50 thousand electron volts (50 keV) in the plasma environment. Because of the different geometry and material properties of the spacecraft surface, different areas on the surface can be charged to different levels. In general, surface charging can be broken down into two types based on the spacecraft's acquired relative potential compared with the potential of its surroundings. The two types of surface charging are frame and differential charging. (Olsen, et al., 1981)

Frame charging, sometimes referred to as absolute or mainframe charging, occurs when the satellite, as a whole, acquires a net potential relative to the ambient plasma. Frame charging is nearly instantaneous, with characteristic periods on the order of micro seconds. Differential charging, on the other hand, takes place when different parts of the spacecraft are charged to different potentials, and it occurs

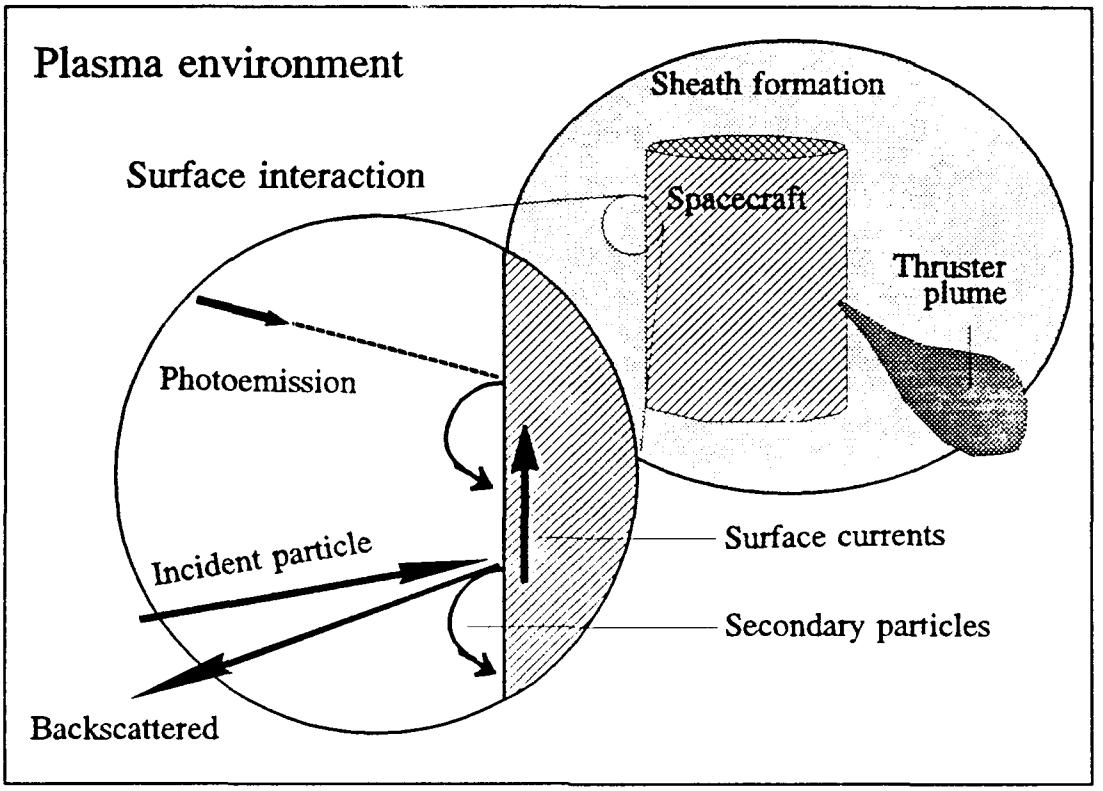

Figure 1. In surface charging, currents from the movement of ambient electrons, ions, secondary electrons, and photoelectrons result in a net current on the external surface of the satellite body. (after Robinson, 1989)

more gradually (with periods on the order of seconds to minutes). Differential charging may produce strong local electric fields, and also can affect the frame charging level of the satellite. From an anomaly effect point of view, differential charging is more significant than frame charging for it can lead to surface arcing or electrostatic surface discharge (ESD) between satellite surfaces of different potentials. This "arcing and sparking" can result in direct damage to spacecraft components and is also known to produce spurious interfering pulses to onboard electronics. (Koons et al., 1988)

In geosynchronous orbit, spacecraft anomalies are often caused by differential charging. Differential charging is particularly common in sunlight, since sunlight tends to keep all illuminated surfaces near the plasma potential, whereas shaded dielectric surfaces can charge to large negative potentials.

Typically, potential differences on the order of one thousand volts are needed to produce an ESD. Each ESD results in an electric arc discharge from regions of high electrostatic potential to regions of lower electrostatic potential and each arc discharge produces an equilibrium redistribution of charge. Arcs generate a transient electromagnetic pulse (EMP), and the EMP can produce undesired signals in electronic circuits, and induce anomalous currents in internal satellite wiring. Both the discharge and the resulting EMP cause satellite anomalies from unintended logic changes in electronics. In geosynchronous orbit, the plasma environment is known to cause differential charging on spacecraft. Anomalies attributable to ESD's, due to surface charging alone, have been known to cause command errors, spurious signals, phantom commands, degraded sensor performance, component failures, and even complete mission loss. A specific example of a severe spacecraft charging event occurred on September 22, 1982 and was recorded by the P78-2 satellite's on board pulse analyzer and surface potential monitor. Three different spacecraft anomalies occurring on that day which were attributed to ESD's. The most serious was a two minute loss of data; the other two were uncommanded mode changes in two experiments. (Koons et al., 1988)

2. Bulk Charging

Bulk or internal charging, also referred to as deep dielectric charging, is the build up of charge on and within dielectric materials or well insulated floating conductors inside the spacecraft. Energetic electrons, with energies from 300 keV to 5 MeV, can penetrate through the surface of the spacecraft and deposit charges inside the Faraday cage of the spacecraft (see Figure 2). (Robinson, 1989, pp. 3-22)

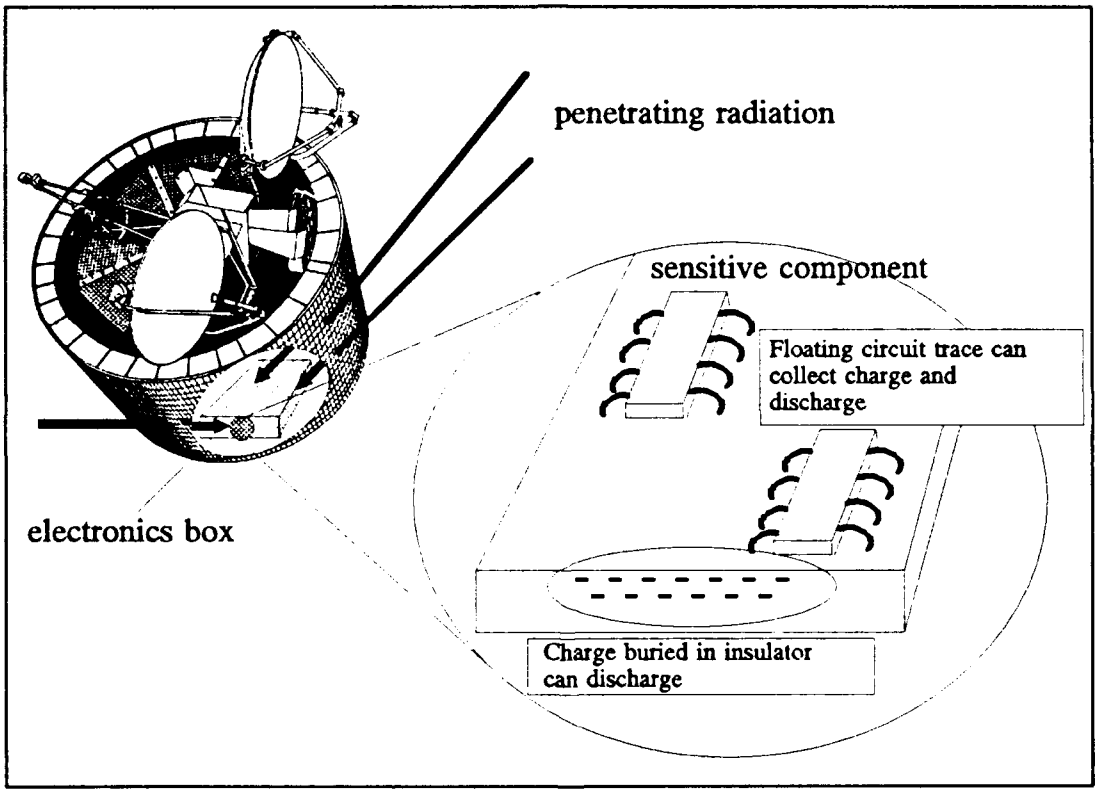

Figure 2. Internal discharge results from charges deposited directly on or in well insulated regions inside the Faraday cage of the spacecraft. (after Robinson, 1989)

Internal charging is dependent on four factors: environment, shielding thickness of the spacecraft, and the characteristics and shape of the charged material. When the rate at which the energetic electrons deposit on the surface or embed

inside a bulk dielectric is greater than the rate at which the charge leaks out, potential will begin to increase in magnitude. Once the generated electric field potential reaches the breakdown value of the dielectric, internal discharge will occur. These internal discharges are known to produce electromagnetic interference or ECEMP, a sharp pulse of electromagnetic energy, which can penetrate into the nearby sensitive electronic components and cause noise, malfunction, or even burn out of circuit boards.

Following the discovery of the surface charging phenomenon, there still remained satellite anomalies which could not be explained by simply invoking the surface charging mechanism -- other charge mechanisms were present. During satellites operation, discharges associated with satellite anomalies, two distinct types of discharges (surface and internal) were recognized. Shaw et al. (1976) categorized these two types of discharge by whether they correlated with the known surface charging mechanism or could not be explained by surface charging. The Voyager I spacecraft experienced 42 power-on-reset (PORs) within the Flight Data Subsystem (FDS) during its passage through the radiation belts of Jupiter. Meulenberg (1976) was first to propose that there was a bi-layer discharge mechanism through the dielectrics within spacecraft. This type of mechanism could possibly explain the observed satellite anomalies that did not correlate with discharges caused only by surface charging.

Leung, et al., (1986) correlated these POR events with the high energy spectrum of particles causing internal charging. Later, after studying the viability of

the internal charging mechanism, Vampola (1987) presented several definitive examples of internal charging at geosynchronous altitude. Of the examples given, the most common cause associated with deep dielectric charging is the deposition in the insulating covers on cables exposed directly to the space environment.

3. Single Event Upset (SEU)

Because of their high energy, cosmic rays cause Single Event Upsets (SEU's) in sensitive micro electronics when spacecraft operate in a radiation environment. "Single Event Upsets occur in micro electronics when a single particle, usually a heavy ion or proton, deposits enough charge at a sensitive node in the circuit to cause that circuit to change state" (Robinson, 1989, pp. 1-9). SEU's cause soft errors (in the sense of wrong bit values) but no damage to hardware. SEU usually takes place in memory, or digital logic which requires information retention as part of its function. Binder et al. (1982) identified specific upsets in "flip-flop" type circuits in the space environment which he attributed to the effect of SEU's.

The basic SEU mechanism involves a single particle passing through the electronic circuit, leaving a track of electron hole pairs. When this track crosses a depletion region, the electric field in the depletion region separates the charges in the track so that the charges do not recombine. If this charge pulse is strong enough and lasts long enough, it can be interpreted by the circuit as a change in state of the bit. This change of state is characterized by a "bit-flip" in memory represented by the circuit. The critical charge concentration the particle must hit in order to cause an upset is determined by the chip feature size. Figure 3 illustrates the SEU

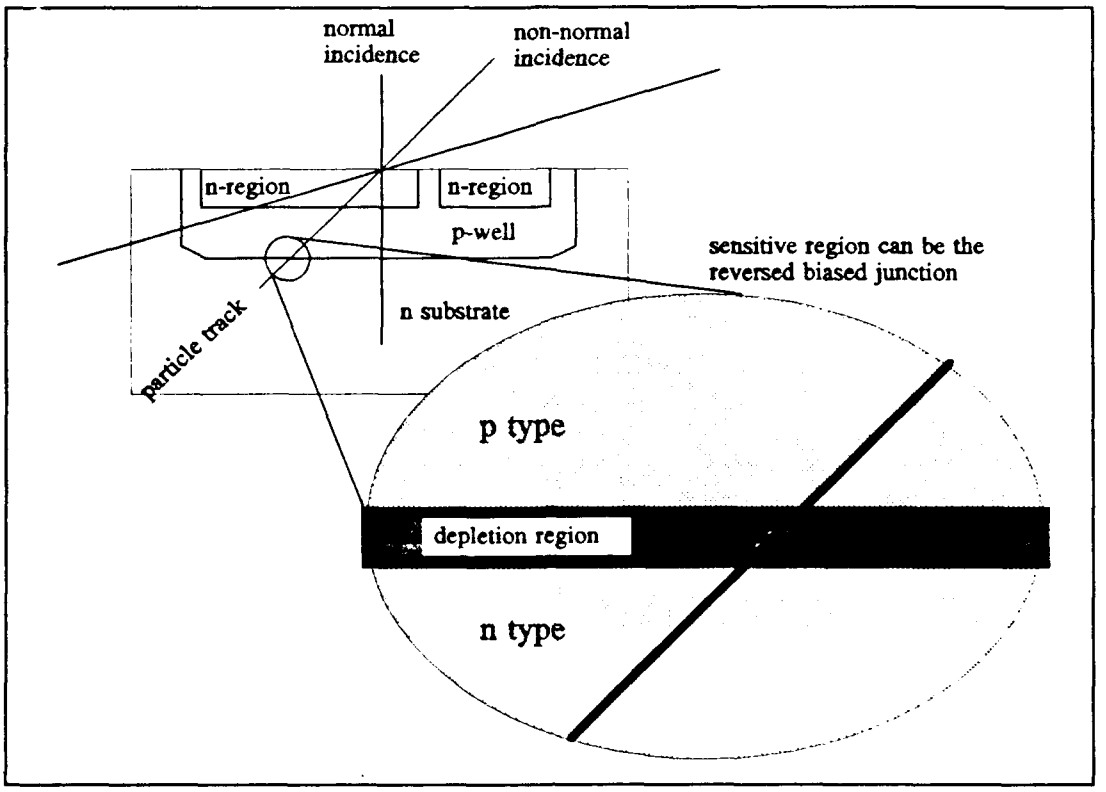

Figure 3. Single Event Upset Diagram (Robinson, 1989, Figure 4-2).

mechanism. The volume the particle must hit to cause an upset is determined by the chip feature size. This sensitive volume determines the cross section or the probability of SEU. Figure 4 illustrates this cross section as the linear energy transfer (LET) of the ionizing particle is varied. LET of the particle is a measure of ability to ionize the material along its path. (Robinson, 1989, pp. 4-4)

As our micro chip technology has advanced in recent years, the performance of Integrated Circuits (IC's) has been improved by increasing both the processing speed and reducing the power requirement for individual circuits. Consequently, these technological advances have required increasingly smaller charge

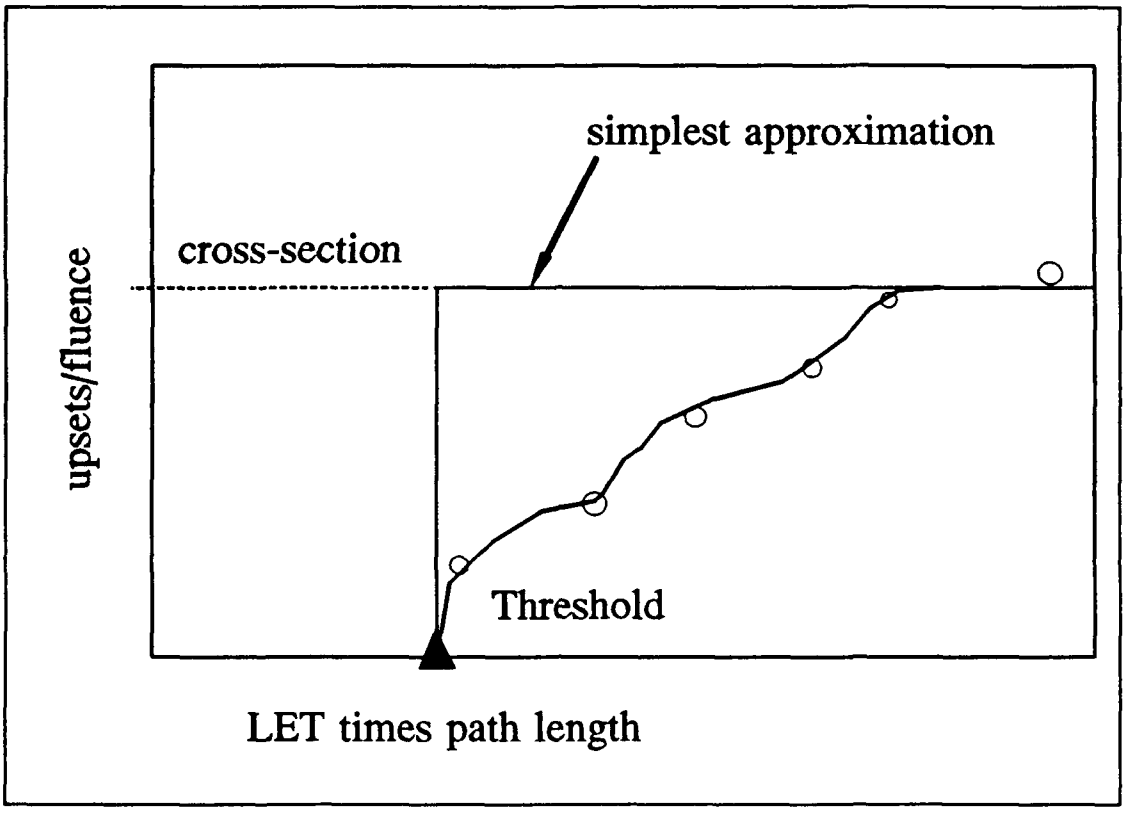

Figure 4. Classical Experiment Cross-Section. The two key parameters for determining the SEU rate are the threshold and the cross-section at large LET times path length. (Robinson, 1989, Figure 4-3).

magnitudes to store comparable quantities of coded information. As a result, each succeeding generation of integrated circuits has become increasingly susceptible to SEU's when spacecraft are operated in the radiation environment. The net effect of the lesser charge dependence for information storage is that smaller disruptions have become more likely to significantly disturb the integrity of integrated circuits.

The higher degree of susceptibility to SEU's is a major concern in designing modern satellites. The SEU rate can be minimized by applying proper passive controls such as better spacecraft engineering designs in conjunction with

hardening programs. Global Positioning Satellites (GPS) provide an illuminating example of the degree of SEU susceptibility modern satellites may experience. GPS anomaly data reported to the anomaly database maintained by the National Geophysical Data Center showed that of the 564 reported anomalies all were directly attributable to SEU's. Bit-flips occurred in the navigation processor, clock register, and telemetry, tracking, and command (TT&C) subsystem. According to Captain Scardera (1991) of the 2nd Space Control Squadron, 2nd Space Wing Operations, U.S. Air Force Space Command who is an engineer working on the GPS project, anomalies in block 1 GPS due to SEU's have not reoccurred in the block 2 satellites after incorporating proper engineering design modifications. For instance, simply increasing the shielding thickness has been an effective method against high energy particles. Figures 5 and 6 are the drawings of the GPS block 1 and block 2 satellites respectively. These drawings illustrate the differences in their surface designs.

The following chapter shall discuss in greater detail the physics behind surface charging and the anomalies caused by ESD's. Chapter three shall analyze anomaly data for several satellites that were caused by surface charging. Finally, from the results of our analysis, the requirement of active charge control for future geosynchronous DoD satellites will be discussed.

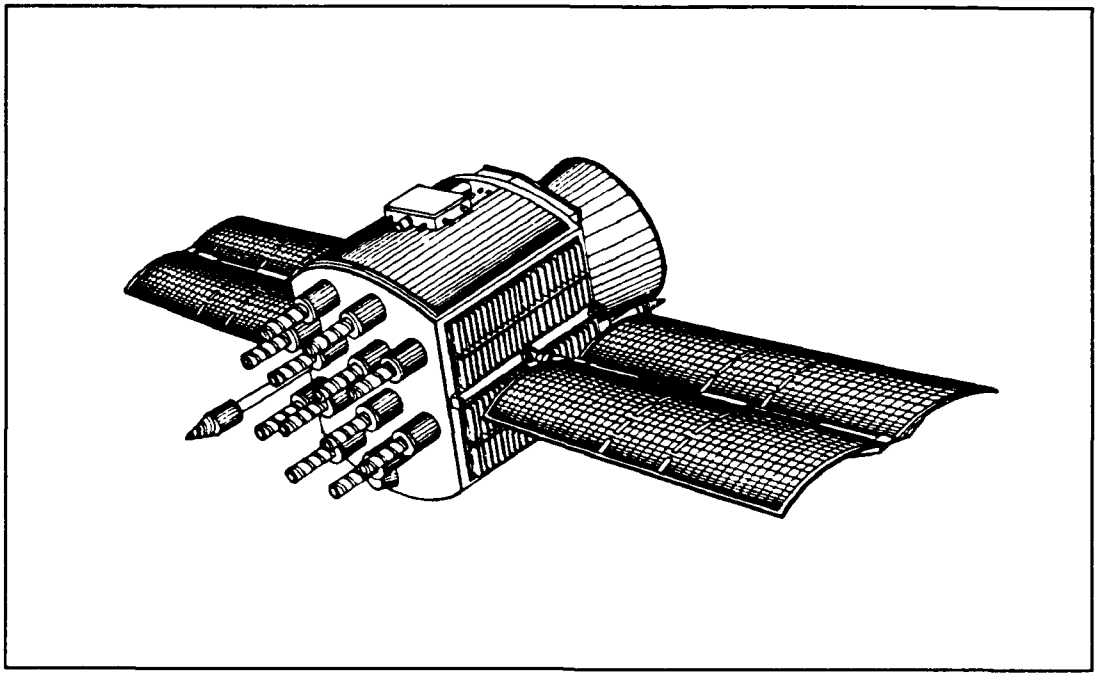

Figure 5. A GPS block 1 satellite.

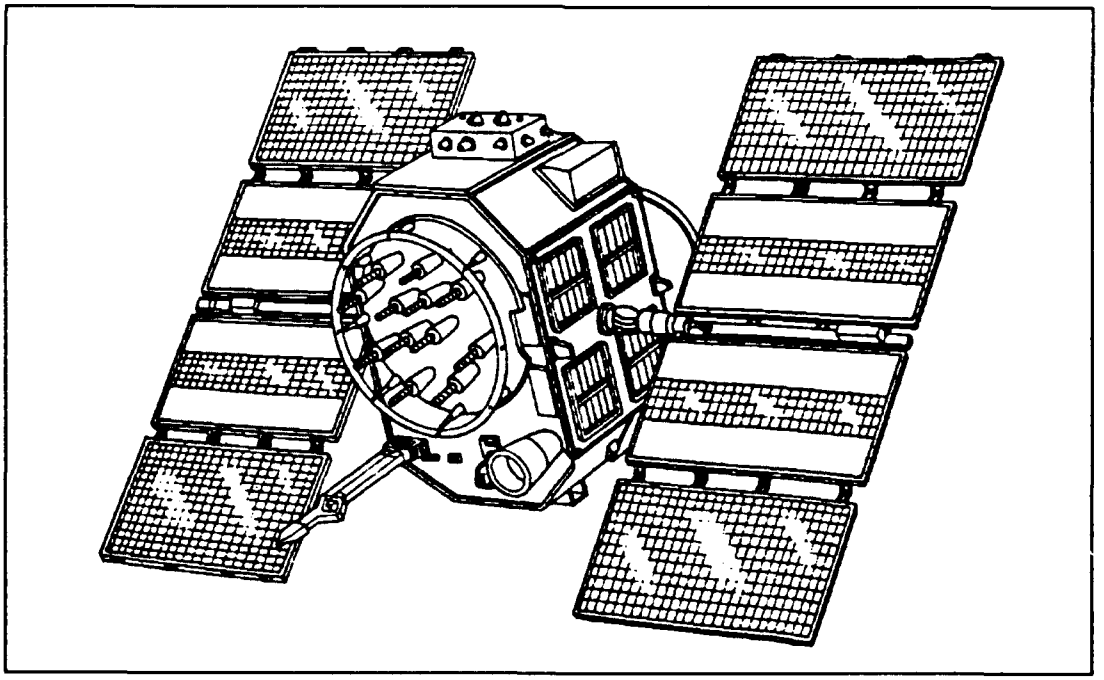

Figure 6. A GPS block 2 satellite.

II. SURFACE CHARGING AND ANOMALIES

A. OVERVIEW

Spacecraft charging often leads to serious operational anomalies (Rosen, 1976). The tendency of modern spacecraft design has been to allow satellites to become larger, and more autonomous. Any functional anomalies are undesirable; for certain satellites missions, **any** anomaly cannot be tolerated. Since both the military and commercial sectors have great interest in spacecraft operations, much work has been done to understand the causes and determine the cures for spacecraft charging. Subsequently, operational solutions have been found for the anomalies once the charging mechanisms and design deficiencies were understood.

Surface charging/discharging is one of many forms of anomaly producing mechanisms. It was discovered on the early space flights. When operating in the space plasma environment, satellites will develop charges on their exposed external surfaces because of interactions between satellites and plasma. In high-altitude orbits, such as the geosynchronous orbit, satellites are greatly affected by space plasma, and surface charging is a major concern. Previously, low altitude surface charging was thought to be insignificant because of low plasma temperatures and high electron densities. However, a recent study conducted by Frooninckx and Sojka (1991) revealed that satellites operating in the upper ionosphere are also affected by the surface charging phenomenon. Defense Meteorological Satellite Program

(DMSP) polar orbiting satellites at an altitude of 840 kilometers (km), can develop and have recorded electric potentials as severe as -1430 volts. These activities are suggested to be related to solar cycles. More research is required on the low altitude surface charging mechanism in order to design charge control systems that will prevent future surface charging related anomalies.

B. SURFACE CHARGING

Surface charging is the phenomenon associated with charge build up on exposed external surfaces of spacecraft as discussed in chapter one. It is a consequence of the interaction between the satellite surfaces and the space plasma, magnetic field, and solar radiation. When a plasma is heated and accelerated towards Earth from the geomagnetic tail region of the magnetosphere, it rushes into the synchronous orbit and bathes spacecraft in hot plasma. Unless the complete outer surface of the spacecraft is conductive and electrically connected, different parts of the spacecraft will be charged to different voltages. At times, adjacent surfaces can be more than a thousand volts apart. The differential charge build up generates an electric field that exceeds a breakdown threshold at some point. This in turn leads to arcing between the surfaces and results in large electrical transients in the spacecraft harness. These transients lead to anomalies in satellite behavior.

C. CHARGING MECHANISM

By definition, space plasma is in a neutral charge state. The net current across an imaginary surface in the plasma environment must be zero so that the overall

charge neutrality of the plasma can be maintained. If the net current flow is not zero, then there will be charge built up on one side of the surface and decrease on the other side. An equilibrium will eventually be established and the net current flow will return to zero after some period of time. Across an imaginary closed surface which is large enough to hold a significant amount of plasma, the net current will be zero. The only requirement for this condition to exist is that an equal number of charges (both positive and negative) flow in opposite directions across the surface (Figure 7).

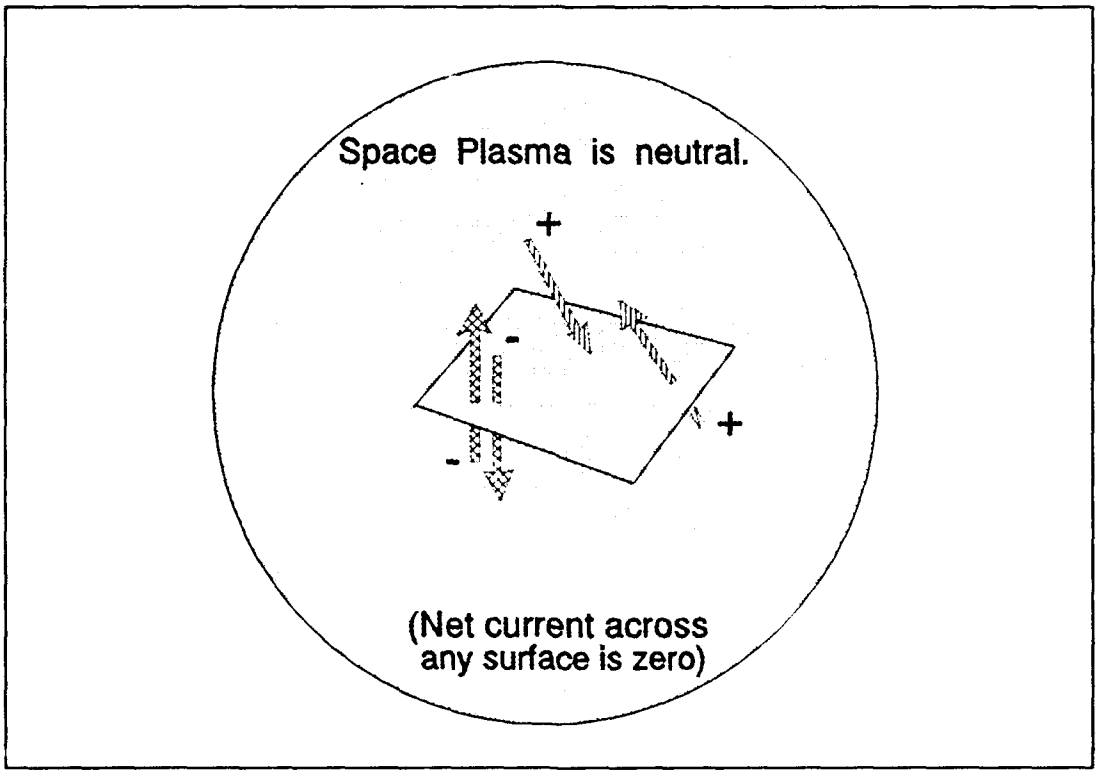

Figure 7. Across any imaginary surface within the plasma, there are an equal number of positive and negative charges flowing in opposite directions across the surface and the net current is zero.

When any solid body (i.e., a satellite) is immersed in the plasma, compensating currents are changed drastically. Charge will build up on the surface of the solid body until an equilibrium between the body and the ambient plasma is reached and the net current flow across the surface becomes zero. During that time, the body accumulates charge, and a sheath is formed. If no discharges occur, the body will eventually reach an equilibrium with the surrounding plasma and the radiation environment so that a surface can be drawn around the body and there will not be any net current flowing through it. The shape and material properties of satellites have much influence over the locations and levels of charges. The potential distribution on and around the satellite can be very complex. (Robinson, 1989)

Consider plasma in a thermal equilibrium state; this state would satisfy the charge neutrality condition of plasma. Within this plasma, for every proton (or electron) traveling in one direction, on an average, there is a proton (or electron) traveling in the opposite direction (see Figure 6). Although the speeds of an electron and proton are vastly different, on the average there are equal numbers of positive and negative charge carriers contained in the imagined volume. When a body, which can absorb charges, is inserted into the plasma, electrons and protons are stopped from reaching the opposite side and charges will be absorbed by the surface of the body.

From the equipartition theorem, the average velocities of the electrons and protons in the thermal equilibrium plasma can be calculated by the following equation:

$$\frac{1}{2}kT=\frac{1}{2}mv^2 \qquad (1)$$

where k is Boltzmann's constant, T is the plasma temperature, v is the average velocity, and m is the mass. Because the proton mass is much heavier than the electron mass, the average electron velocity is much greater than the average proton velocity. Since the current is proportional to the average velocity and charged particle density, assuming it is the same for both charged particles in the plasma, the electron current will flow to the surface of the body at a higher rate than the proton's. A negative charge potential will build up on the body surface (Figure 8). This process will continue until the electric field produced by the accumulation of

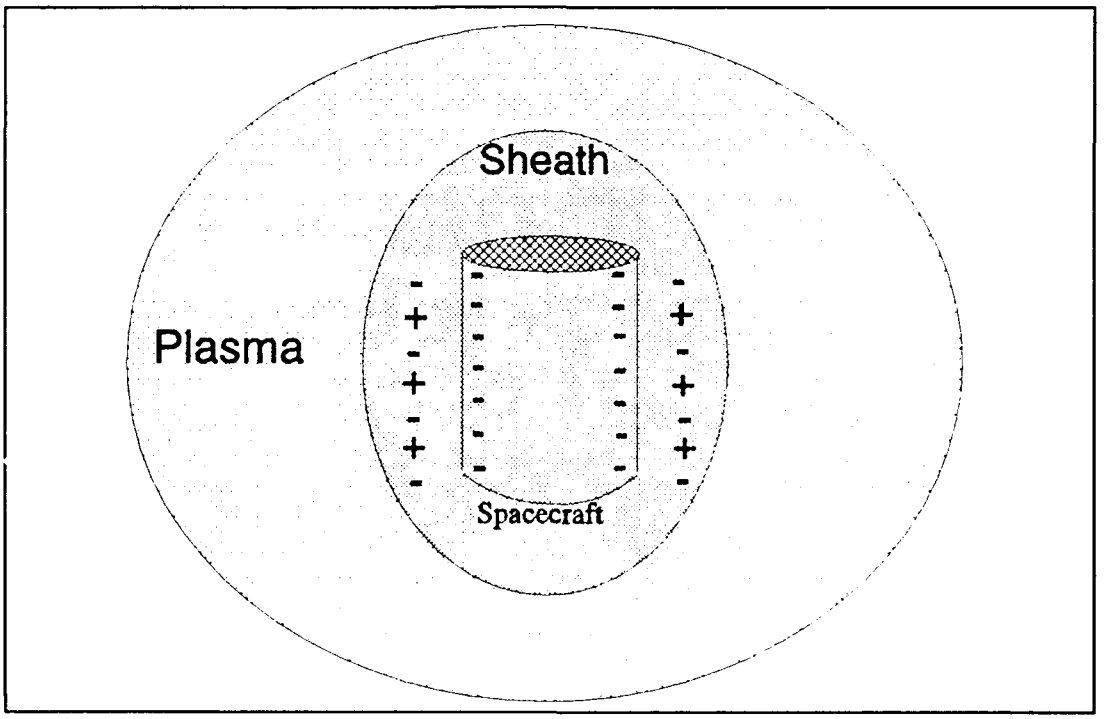

Figure 8. Since the average velocity of the electron is faster than the proton's, the electron current is flowing to the surface of the body at a higher rate than the proton. Therefore, the surface is charged to a negative potential.

charge is strong enough to repel electrons and attract positive ions. Eventually, an equilibrium condition will be reached when the net current to the surface reaches zero.

Spacecraft surfaces are made of different shapes and materials of various characteristics. Typical conducting materials are aluminum, or conducting paint; typical insulating surfaces are the glass covers of silicon solar cells, and the kapton used for thermal blankets. Since these materials possess different electrical properties, it is a complex system to analyze. Surface (material) properties determines photoelectric yields, and secondary emission yields. When electrons or ions impact on a surface, one or more electrons will typically be emitted from the surface. This effect is called secondary emission. Secondary emission, which depends on the material plays an important role in determining the net current to the surface.

D. DEBYE LENGTH

In plasma physics the parameter which describes the distance over which an electric field exists in the plasma is the Debye length (λ) in meters.

$$\lambda = \sqrt{\frac{\epsilon_0 kT}{\eta_e e^2}} = 69\sqrt{\frac{T}{\eta_e}} = 7430\sqrt{\frac{kT}{\eta_e}} \qquad (2)$$

where ϵ_0 is the permittivity constant, k is the Boltzmann constant, T is temperature of the electrons in degrees Kelvin, η_e electron density, e is the electronic charge, and kT is the plasma temperature in eV. When a spacecraft is at high altitude, 5 to 7 earth radii (R_e), the Debye length is large compared to the dimension of the

spacecraft. Individual particle trajectories are controlled by the electric and magnetic fields near the spacecraft. As an example, consider a typical case in the magnetosphere where the plasma temperature, kT, is approximately 8 keV and the electron density, $\eta_{e,}$ is 10^6 [e/m^3]. From Equation (2), the Debye length λ is equal to 665 meters, which is considerably larger than typical spacecraft dimensions. Because of this, the electrons envelop the vehicle with a distribution similar to the "vacuum" solution of Laplace's equation ($\nabla^2\phi = 0$).

In contrast, at low altitudes, i.e., at Low Earth Orbit (LEO), or when the velocity of the spacecraft is high compared to the thermal velocities, the Debye length is short compared to the spacecraft and the particles trajectories are strongly influenced by the presence of the plasma sheath around the vehicle.

E. WAKE EFFECT

Spacecraft in low altitude earth orbits have orbital velocities on the order of 7 km/sec. At altitude of 1,000 km, the thermal velocities of the ambient ions is 3 km/sec for H^+ and 0.8 km/sec for O^+. The movement of a spacecraft through the ionosphere produces a wake. It takes a finite time for the ions to fill in the void created behind the passing spacecraft. The electron thermal velocity at that altitude is 180 km/sec. The electrons tend to fill in the void but are retarded by the electrostatic field that results from charge separation at the wake. (Robinson, 1989, pp. 2-40)

F. CURRENTS

Since charged particles are moving, they can be treated as currents; the equilibrium potential of the spacecraft can be determined by the balance of currents. The currents to a surface in space must be balanced at an equilibrium, otherwise charge will build until current balance is attained. The principal charging currents are due to the ambient electrons and the emitted photoelectrons.

The space environment is the main factor in determining currents to and from the surface of the spacecraft. In a plasma environment, the density of the plasma determines the type of current flowing to the surface. The current density also affects the radiation induced conductivity which in turn affects the leakage current throughout the material. This latter effect is important for dielectric charging. When in equilibrium, if the surface is conducting, all currents to the connected conducting surfaces sum to zero. Or if the surface is insulating, the net current to each point on the surface is zero. The primary current is directly proportional to the plasma density, and can be expressed as:

$$j = nqv_{average} \tag{3}$$

where j is the primary current of charged particles, n is the density of surrounding plasma, q is the charge on a particle, and $v_{average}$ is the average velocity of the particle. With the same velocity distribution, plasma of greater density will charge the spacecraft and its surface more quickly than a plasma of lesser density.

Referring back to Figure 1, the net current to a surface is the sum of currents due to ambient electrons and ions, secondary electrons, and photoelectrons. To calculate the spacecraft potential, the current balance equation can be written as:

$$I_{total}=I_e+I_i+I_{e/e}+I_{e/i}+I_{bs}+I_{photo}\pm I_{other} \quad (4)$$

where the I_e and I_i are the primary electron and ion currents from the plasma to the surface. The $I_{e/e}$ and $I_{e/i}$ are the secondary emission currents due to incoming electrons and ions respectively. I_{bs} is the current of electrons leaving the surface due to backscattering electrons. The I_{photo} is photocurrent resulting if the surface is exposed to photons. In most space charging environments, the largest current interacting with the spacecraft surface is from photoemission. Photoemission has been characterized in a way similar to secondary emission; it depends on the characteristics of the surface material. Finally, the last term, I_{other} represents any other current which has not been mentioned. This may include current due to Ohm's law current from spacecraft, thruster operation, ion engine current, wake effect, or anything else. At equilibrium, $I_{total} = 0$, if the "environment" not changing.

G. ANOMALIES

If one had to define the word "anomaly" associated with spacecraft, in the simplest term, an anomaly is any unscheduled, undesirable event occurring to the spacecraft. An anomaly can range from a simple data bit error to a total mission failure. The most common type of anomaly is the phantom command. Phantom command causes satellites to perform a task which it was not given intentionally as

part of the operations. The two minute loss of data onboard P78-2 satellite given on page 6 is an example of phantom command caused anomaly.

The remainder of this section provides examples of surface charging related satellite anomalies. In these examples, satellites experienced various degrees of subsystem on orbit malfunctions, and their mission performances were directly impaired. Although these satellites were not properly designed to exclude environmental effects, they should be looked upon with gratitude for their pioneering works rather than as failures due to poor engineering designs.

1. DSCS

The first major satellite system to have environmental problems was DSCS, a military communications satellite. The complete mission failure of the first DSCS drew a great deal of speculation as to the cause of the failure. DSCS-1 was launched on November 11, 1971 into geostationary orbit. Figure 9 is a drawing of the DSCS satellite.

The original failure report is no longer available, however, the failure characteristics have been obtained from Aerospace Corporation, courtesy of Dr. Harry Koons. The Orbit Data Acquisition Program (ODAP) is a depository of on-orbit incidents maintained by the Aerospace Corporation in Los Angeles, CA.

The failure of DSCS-1 was attributed to a geomagnetic storm. The failure report stated that within the electrical power and distribution subsystem, there was a power interface switching mechanism to work the load control assembly. This power interface switch failed and there was no power available to the

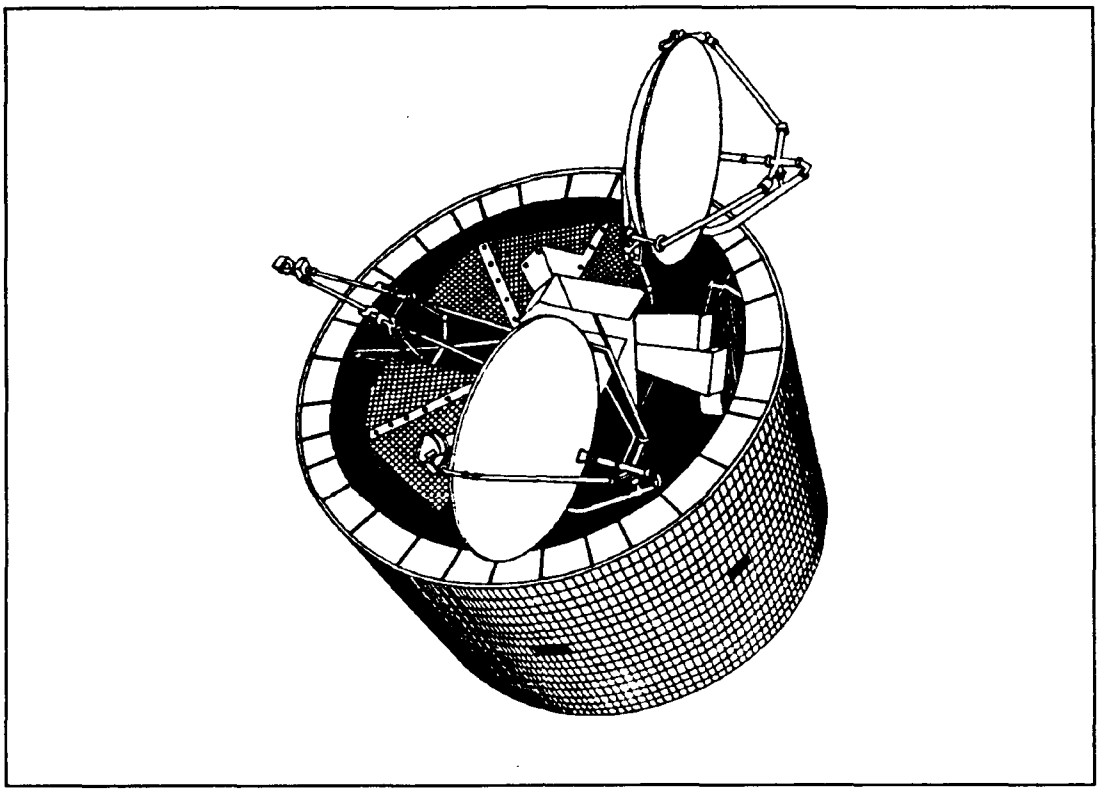

Figure 9. A DSCS satellite.

communications subsystem. This caused the mission to be terminated because the switch logic assembly commands were ineffective in correcting the problem. The failure was attributed to ESD. The ESD was a result of charging induced by the enhanced electron flux associated with a geomagnetic storm. The report recommended that all (where possible) external conductive surfaces be properly grounded in all future satellites to eliminate differential charging during geomagnetic storms. (Koons, 1991)

2. CTS-Hermes

An early experiment designed to study satellite anomalies was to place the Transient Event Counter (TEC), on the joint Canadian-American Communications Technology Satellite (CTS). CTS, called Hermes, was launched on January 17, 1976 from Cape Canaveral by a Delta rocket and placed into geostationary equatorial orbit at 116° West Longitude. Hermes was designed to test three technologies: (1) transmission at 12-14 GHz, (2) on orbit deployment of light solar cell panels, and (3) three axis stabilization. Figure 10 is a drawing of Hermes.

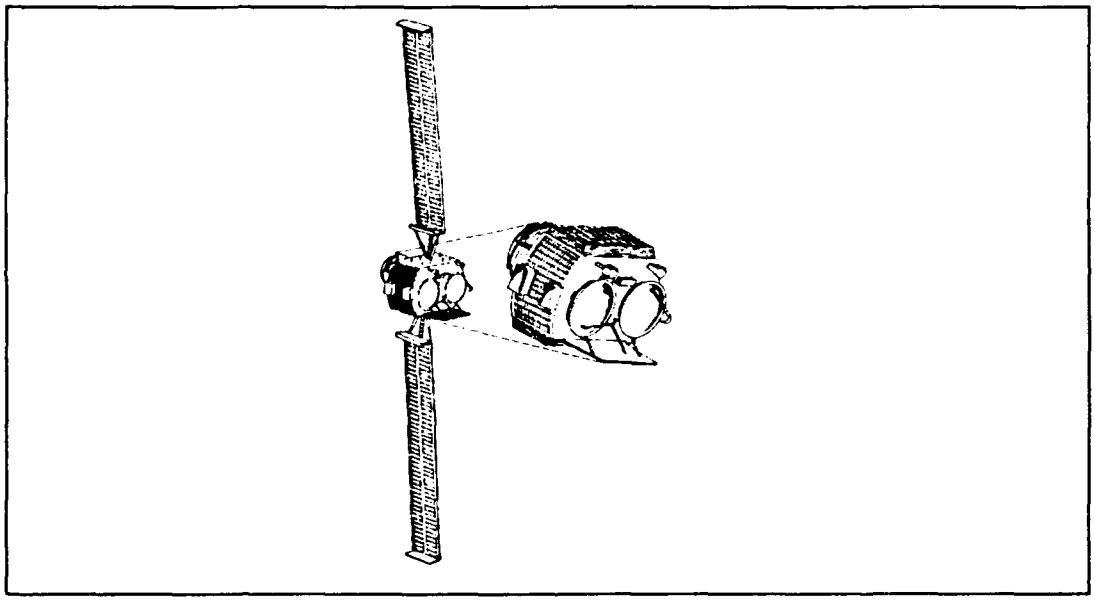

Figure 10. Communications Technology Satellite (CTS), Hermes.

The purpose of the TEC was to identify transients in the spacecraft wiring harnesses which could be attributed to the spacecraft charging phenomenon. It was designed to sense and count electrical transients which exceed 5 volts in amplitude at rise times of less than 0.3 μsec which could cause switching of spacecraft logic

circuits. Stevens and Klinect (1977) studied the data collected by the TEC during the first year of its operation. In the data there were 215 transient events detected in the system wire harnesses which were presumably due to spacecraft charging events. All satellite data had been verified to the fact that no commands were being executed and there were no power fluctuations concurrent with the TEC-sensed transients. Among the data, 65 percent were multiple transients. The cause, as explained by Stevens and Klinect (1977), was that the large insulator areas on the satellite did not discharge all at once. Rather, a discharge occurred in one region which in turn triggered discharges in another area. Also, the data showed that the distribution of the events appeared to be random; satellites could be charged by the geomagnetic substorm environment at about local midnight, but the discharge might not occur for several hours.

There was a part failure on Hermes as well. On June 8, 1976, an anomaly that was induced by spacecraft charging occurred. A short circuit took place on the experiment power bus. The short lasted 24 seconds, and it caused the power bus to burn out. The most probable location of the short was at the power insulating diodes which were exposed to the environment; a moderate substorm was recorded a few hours preceding the short.

3. P78-2, SCATHA

Following the DSCS accident, a complete mission failure, a massive effort to understand the source of the anomaly was initiated (Robinson, Jr, 1989, pp. 1-2). One part of this effect was the launch of the P78-2 spacecraft, the Spacecraft

Charging At High Altitude (SCATHA) program. The United States Air Force P78-2 satellite (SCATHA), see Figure 11, was launched on January 30, 1979 with 27° inclination angle, 185 km perigee, and 43,905 km apogee. The SCATHA spacecraft had two initial objectives: to measure the charging characteristics and material effects (Shane, 1977). Other elements of the SCATHA program included ground experiments, and development of computer models for surface charging on spacecraft. The experimental equipment onboard P78-2 are listed in Table I.

Table I. The experimental equipment onboard P78-2 satellite.

IDENTIFICATION	TITLE
SC1	Engineering Experiment Plus VLF and HF Receivers
SC2	Spacecraft Sheath Fields Plus Energetic Ions
SC3	High Energy Particle Spectrometer
SC4	Satellite Electron And Positive Ion Beam System
SC5	Rapid Scan Particle Detector
SC6	Thermal Plasma Analyzer
SC7	Light Ion Mass Spectrometer
SC8	Energetic Ion Composition Experiment
SC9	UCSD Charged Particle Experiment
SC10	Electric Field Monitor
SC11	Magnetic Field Monitor
ML12	Spacecraft Contamination Plus Thermal Control Materials Monitoring
TPM	Transient Pulse Monitor

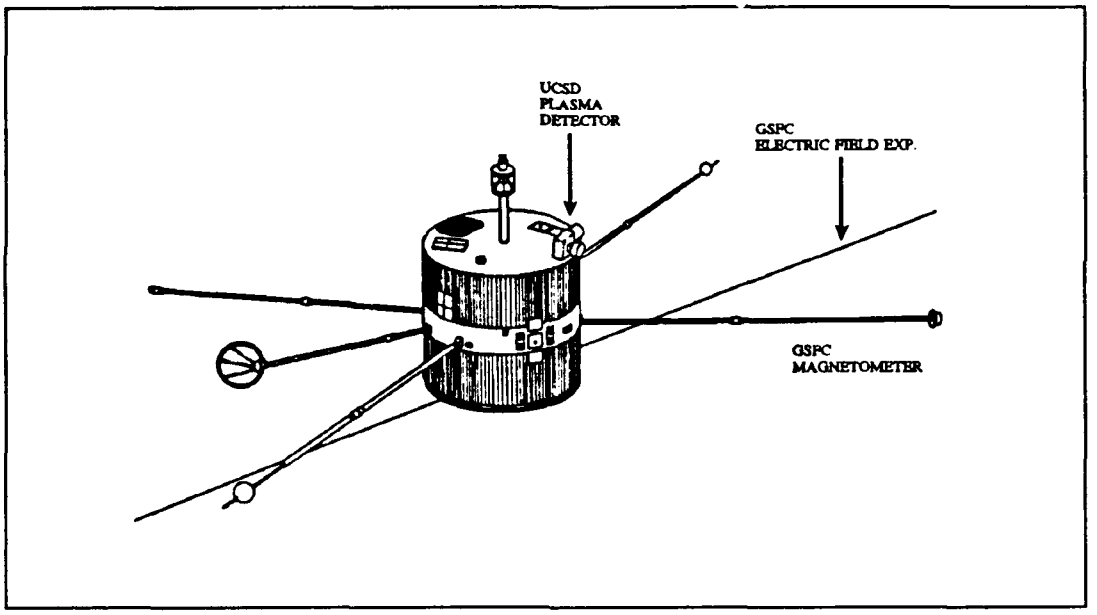

Figure 11. The P78-2 SCATHA satellite.

With the successful flight of the P78-2 satellite, a great deal has been learned about surface charging from data collected by instruments on board the P78-2. These data validated that there is a close tie between surface charging and the space environment.

On September 22, 1982, a large number of intense electrostatic discharges were detected by the engineering instruments aboard the P78-2 satellite. In only one day, the Pulse Analyzer detected 29 pulses; 17 of the pulses exceeded the maximum voltage discrimination level which was set to 7.4 V. The Transient Pulse Monitor also detected 29 pulses and most of them were coincidental in time with those detected by the Pulse Analyzer. During the same time period the satellite Surface Potential Monitor experiment measured the largest differential surface charging observed in the data analyzed since launch. The gold sample voltages exceeded -300

V on four separate occasions. Each time the voltage exceeded this value, ESD's were recorded by the Pulse Analyzer. Three different spacecraft anomalies occurred on P78-2 on that day. The most serious was a two minute loss of data. The other two were uncommanded mode changes in two experiments. (Koons et al., 1988)

a. Two Minute Data Loss

A two minute period was missing from the tape-recorded data of the satellite. Although no pulse was recorded near the two minutes when data were missing by the pulse detectors, the signature of a pulse appeared in the data from the Very-Low-Frequency (VLF) Wave Analyzer experiment. Each pulse detected by the Pulse Analyzer also produced an anomalous output from the VLF experiment. It was believed that the discharge caused the pulse code modulation subsystem to lose synchronization.

b. State Change in Magnetic Field Monitor

A filter select relay in the Magnetic Field Monitor experiment occasionally changed state. This occurred during the time when discharges were occurring on the vehicle. One such filter state change occurred on September 22, 1982.

c. Timing Errors in VLF Plasma Wave Analyzer

Anomalous timing errors occurred in the VLF Plasma Wave Analyzer. The VLF experiment collected data from two sensors, an electric antenna and a magnetic antenna. The experiment contained a counter that counted the Main

Frame sync pulses from the telemetry system. The pulses occurred at the rate of one per second. At every 16 sync pulses the antenna was switched. The anomaly that occurred on September 22, 1982 was a failure of the antenna to switch properly after virtually every discharge. The switching failures coincided with four of the discharge pulses in the two minute data loss period. (Koons et al., 1988)

4. METEOSAT

METEOSAT-F1 (Figure 12) suffered from a number of non-damaging operational anomalies that were attributed to ESD's caused by differential charging. Phantom commands, mentioned on page 24, are now illustrated by the switching problem METEOSAT-F1 encountered.

In 1972 the European Space Agency (ESA) initiated the program for the development of two pre-operational meteorological satellites to be put in geostationary orbit. METEOSAT-F1 and F2 were the meteorological spacecraft, built and operated by the ESA to provide meteorological data to weather forecasting agencies in the European sector. METEOSAT-F1 was launched in November 23, 1977, and was furnished with a high-resolution radiometer which takes pictures in three spectral bands: the visible, thermal infrared, and water vapor bands. The radiometer was an electro-optical instrument with a 40cm diameter telescope and was capable of providing two images of the Earth in the visible and infrared wavebands every 25 minutes.

On November 24, 1977 METEOSAT-F1 experienced inadvertent stop of radiometer scanning soon after operations had begun. The cause of the anomalous

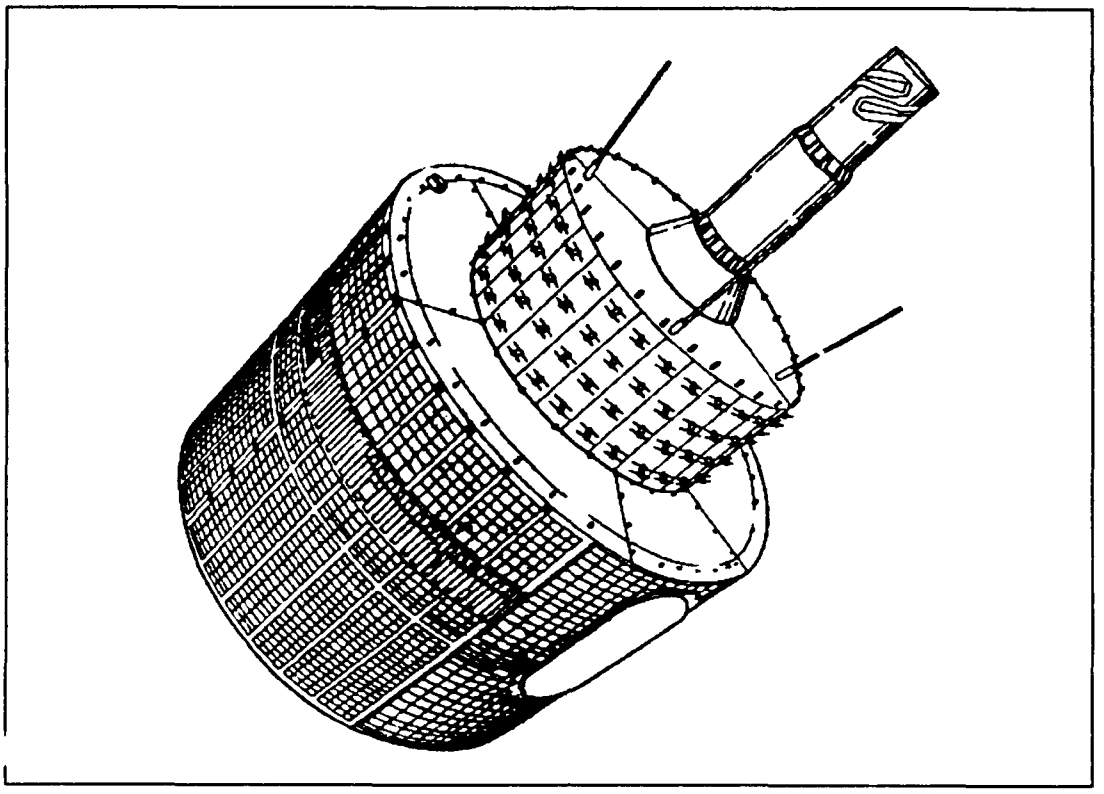

Figure 12. A METEOSAT satellite.

status change was traced to a few sensitive circuits. Robbins (1979) studied the Meteosat F1 anomalies and found that anomalies were more common at times of high geomagnetic activity. In three years of operation Meteosat F1 experienced over 150 anomalies. Hoping to correct the problem, the following two design improvements were incorporated into the building of METEOSAT-F2:

- grounding of the outer layer of the thermal shields in order to avoid high potential build up on those surfaces.
- Replacing electronic circuits by relays in the radiometer stops circuit in order to increase the level of energy needed to trigger the radiometer stops. (Hoge, 1982)

METEOSAT-F2 was launched on June 19, 1981. The number of anomalies was dramatically reduced. The decrease was attributed to the design improvements. (Johnstone, et al., 1985)

5. SMS-GOES

After the testing of several meteorological instruments aboard the ATS-1 and ATS-3 satellites in geostationary orbit (the first satellites in geostationary orbit), the first American geostationary meteorological satellite was launched in 1974. It was named Synchronous Meteorological Satellite (SMS). Subsequent flights were named as Geostationary Operational Environmental Satellite (GOES). The first GOES-4 was launched on September 9, 1980, and GOES-5 was on May 22, 1981. The GOES-4 (Figure 13) and -5 also suffered phantom command effects with their Visible and Infrared Spin Scan Radiometer (VISSR) subsystems.

The principal onboard instrument, an atmospheric sounder, was the VISSR. This instrument observed the earth using the spin of the spacecraft to scan in the east-west direction. A mirror was stepped to produce scans in the north-south direction. There were eight channels of data taken in both visible and infrared regions of the spectrum.

The VISSR subsystems aboard GOES-4 and -5 had shown instances of anomalous changes in its state corresponding to false commands. There were 13 anomalous commands recorded during a 15 month period from November 1988 to March 1990 for GOES-4, and 14 anomalous commands in a six month period from October 1989 to March 1990 for GOES-5. The first anomaly observed on GOES-4

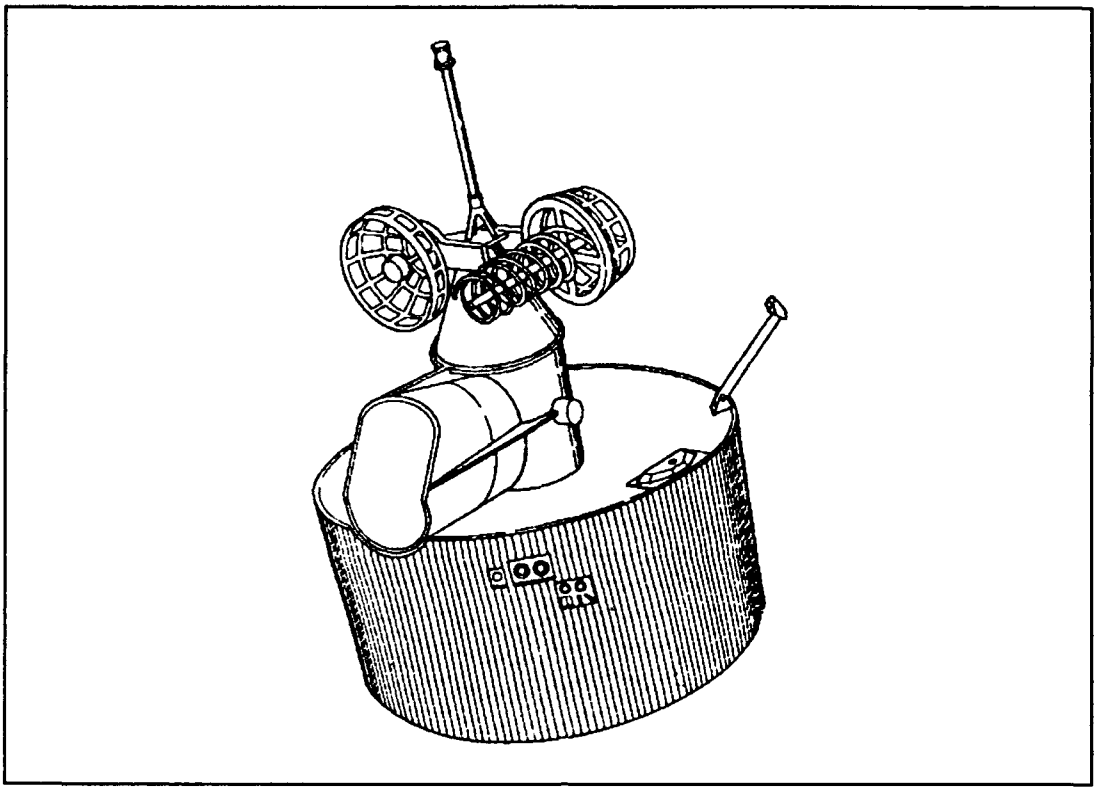

Figure 13. A GOES-4 satellite.

on March 29, 1981 was an uncommanded stepping of the VISSR mirror. At the same time, the gain in one of the visible channels (Ch 6) had an uncommanded gain step. On April 1, 1981, the mirror again began uncommanded stepping. Ground magnetograms examined shortly after these anomalies showed evidence of substorm activity, suggesting that these anomalies were environmentally induced. (Robinson, 1989, pp. 5-7)

A search for the cause revealed that part of the VISSR second stage radiation cooler was ungrounded. The inner member of this assembly was grounded through a wire which went into the VISSR electronics package. It was proposed that charge built up on the ungrounded radiator until a breakdown occurred across the

insulating epoxy bonding the two parts together. The resulting current surge was then conducted through the ground wire into the VISSR electronics. Tests performed on the GOES-5 spacecraft which at the time was awaiting launch confirmed that the radiator was indeed ungrounded. GOES-5 was modified to ground the radiator, and did not experience this particular command anomaly again. (Robinson, 1989, pp. 5-7)

6. MARECS-A

In December 1981, MARECS-A, an ESA's telecommunication satellite, shown in Figure 14, experienced some unexpected spurious switching problems soon after launching. Most (65 percent) of these spurious switching problems were harmless triggering of telemetry latches. However, a more serious impact on the operation of the satellite was caused by uncommanded triggering of back-up functions for the attitude control since it could disturb the communication traffic. (Lechte, 1986, pp. 24-2)

MARECS-A anomalies showed a seasonal variation; most of them occurred around the equinoxes. There was a good correlation between observed MARECS-A spurious switchings anomalies and the distribution of sunspot numbers as measured by the A_p-index over a year (Lechte, 1987). Figure 15 shows there was a good correlation between MARECS-A anomalies (in the period between 1982 and 1985) and the diurnal variation of the electron flux as measured on SCATHA and ATS-5. There seems to be a delay between the maxima of the flux and spurious switchings. In early 1982, the onboard safety mode "Emergency Sun Reconfiguration

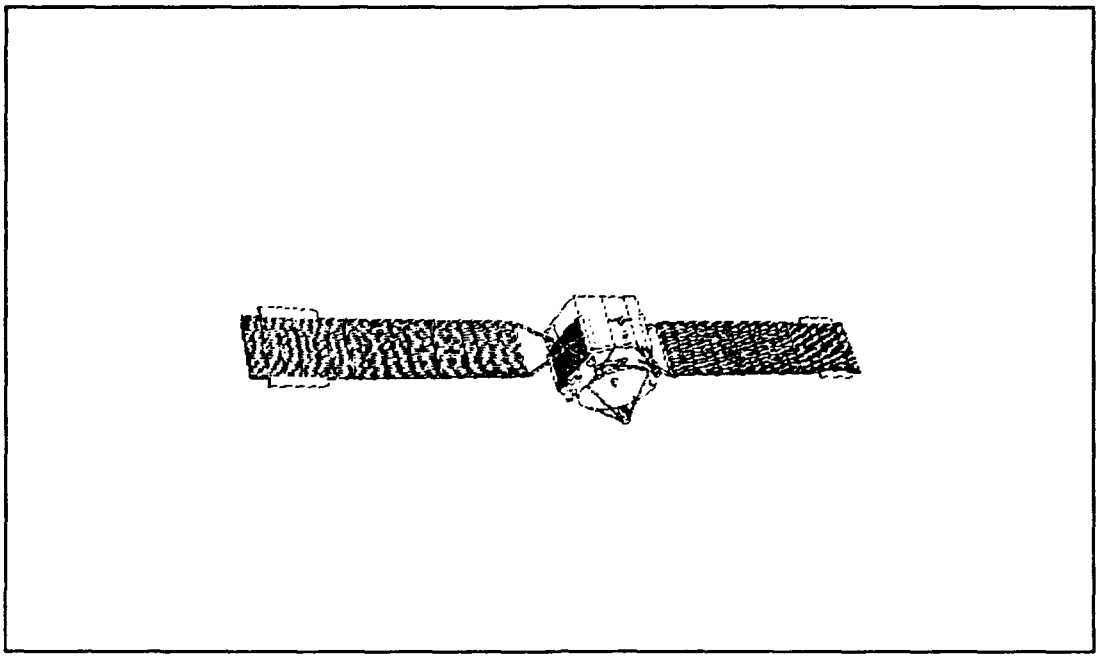

Figure 14. MARECS-A satellite.

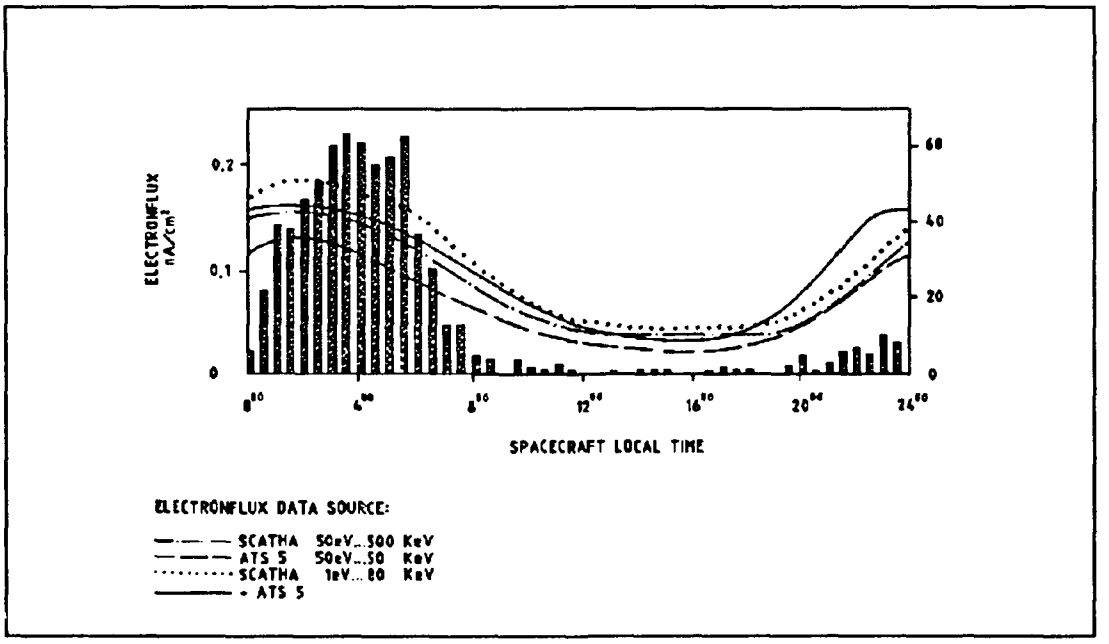

Figure 15. Diurnal distribution MARECS-A spurious switchings and electronflux. (Lechte, 1986, pp. 24-3)

(ESR)" actually temporarily interrupted the communication link. After this anomaly, ESA decided to investigate the reasons for the spurious disturbances on MARECS-A. The investigation concluded that most of the spurious switchings were caused by ESD's. The findings would be implemented into the future satellite design in order to eliminate the switching problem on subsequent MARECS-A satellites. (Lechte, 1986, pp. 24-3)

7. Anik D

Canadian geosynchronous domestic satellites, Anik D (Figure 16), were built by SPAR with Hughes as their bus and reaction control system supplier. Anik D1 and D2 were launched in August 1982 and November 1984 respectively. Numerous observed anomalies occurred on Anik series satellites which were caused by phantom commands. One rather serious event which took place onboard Anik D led to a temporary loss of control of the satellite and a consequent loss of fuel. Anomalies were believed to have been caused by electrostatic discharges, and the thermal blanket was considered to be the primary source of ESD. (Wadham, 1986)

Anik satellite anomalies were studied by Wadham (1986). He pointed out that on March 8, 1985 the Anik D2 despin control system malfunctioned and the despun platform suddenly spun up. There was a temporary loss of all telemetry data since these data were transmitted via the communications antenna which was mounted on the despun platform. Wadham thought this anomaly was a unique occurrence because of the following events had taken place simultaneously:

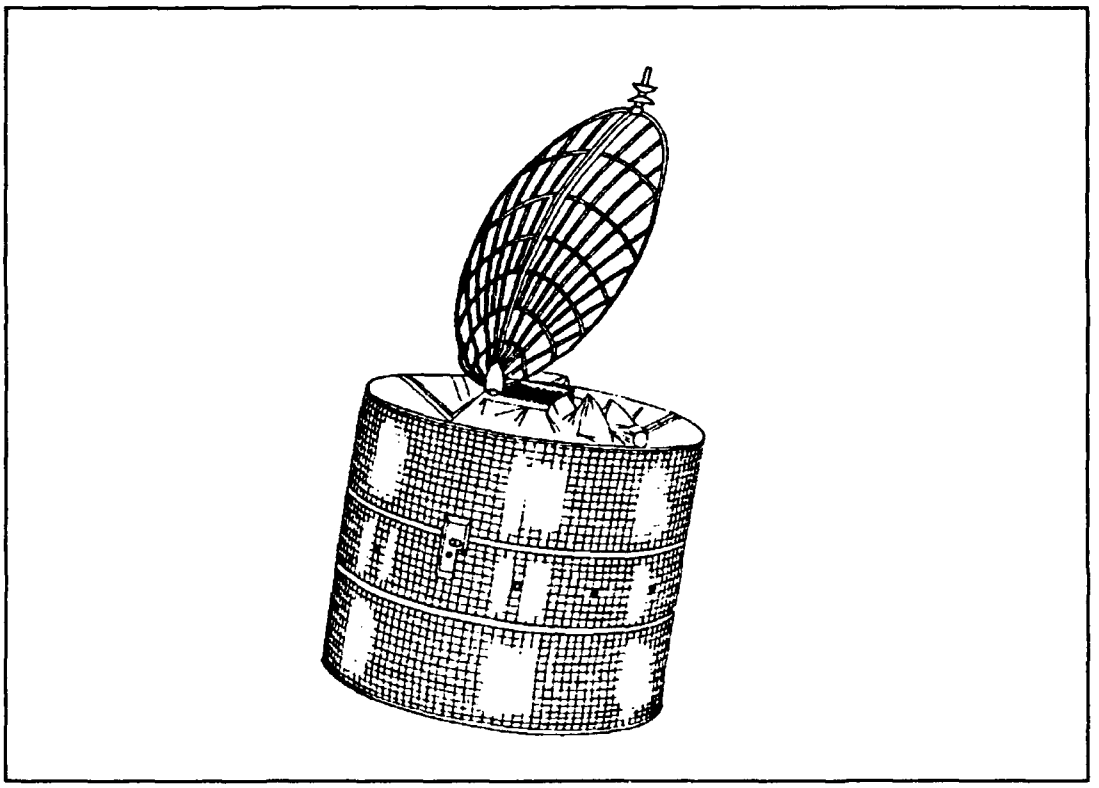

Figure 16. Anik D satellite.

- A change in status of the logic which told the despin control system whether or not the command receivers were locked to the pilot uplink.
- The disabling of logic circuitry intended to indicate to the despin control loop any loss of the pilot signal.
- The disabling of logic circuitry intended to indicate if the earth sensors were no longer pointing at the earth.
- The switching of logic circuitry controlling the earth sensor selection, from the North sensor to the South sensor.
- The resetting of the timing of one of the telemetry subcommutators.
- The catastrophic failure of one of the redundant telemetry encoders.

Wadham indicated if only two of the first three events had occurred, the satellite would not have spun up. The control system could not cope with the three events occurring simultaneously. Wadham postulated that a large arc discharge occurred; it originated at the thermal wrap on the back of the communications antenna reflector or at the thermal shield on the front.

Wadham (1986) also pointed out that prior to and up to the time of the event, there was unusually high geomagnetic activity in the magnetosphere. Immediately after the event, the activity became very low and remained at a low level for several days thereafter. Because the despun section was dynamically unbalanced due to the antenna offset, the spin-up caused the satellite to wobble, and in turn caused a nutation control thruster to fire. The net result was a loss of fuel equivalent to about a year of stationkeeping. (Wadham, 1986)

H. ANOMALIES AND SOLAR ACTIVITIES

When the space environment lacks lower energy particles, and is rich in electrons with energies above one keV, surface charging and discharging will occur. This usually happens during magnetic substorms or solar particle events. Electrical discharges on surfaces of geosynchronous spacecraft due to differential charging were reported to occur at higher rates during periods of increased geomagnetic activity. The SCATHA satellite which was launched in 1979, on one occasion had a kapton sample negatively charged to 3 kV in concurrence with several orders of magnitude change in electron flux during a substorm expansive phase (Reagan, et al., 1981).

Allen (1991) studied the solar and geomagnetic activities which took place during March, 1989. A list of the consequences for space systems was given. They included:

- GOES-7 communications circuit anomaly, lost imagery, and communications outage
- Three low altitude NOAA polar orbiting weather satellites and the USAF DMSP had trouble unloading torque due to the uncommonly large ambient magnetic field changes.
- Japanese geostationary communications satellite CS-3B had failure and permanent loss of half of the dual redundant command circuitry on board.
- A series of seven commercial geostationary communications satellites had considerable problems maintaining operational attitude orientation within specified ranges.
- The Japanese geostationary meteorological satellite GMS-3 suffered severe scintillations; Data transmissions were lost for about one hour.
- Geostationary communications satellites reported operational anomalies.

Historically major flares increased magnetic storms on Earth, causing power outages and disrupting electromagnetic communications. Between December 20-30, 1990, 16 major solar flares were reported (Lancaster, 1991). This period of heightened solar activity raised concerns about the reliability of space based military support for operations (Desert Shield) in the Mideast during the following months. It was felt that these solar activities might severely disrupt military communications and satellite surveillance.

III. ANOMALY ANALYSIS

A. ANOMALY DATA SOURCES

The Solar-Terrestrial Physics Division of the National Geophysical Data Center (NGDC) in Boulder, Colorado maintains a Spacecraft Anomaly Database. In this thesis, it will be referred to as the NGDC database. Each entry includes the date, time, location, and other pertinent information concerning incidents of spacecraft operational disorders attributable to the space environment. The NGDC database covers the period from July 1973 to April 1989 (6652 days) and contains 3387 entries from 24 different satellite types. The NGDC supports retrospective data requests and analysis. The NGDC also accepts anomaly data directly from satellite operators to keep the database current.

A second set of data was helpfully provided by Captain Scardera of the 2nd Space Control Squadron, 2nd Space Wing Operations, U.S. Air Force Space Command, in the form of operational anomaly reports on the GPS's for the period from July 1989 to March 1990.

B. SPACECRAFT ANOMALY MANAGER (SAM)

The NGDC's anomaly database is maintained in dBASE III type files for IBM compatible computers. The Spacecraft Anomaly Manager (SAM) is a custom built software package developed to facilitate database access. The SAM performs a full

range of functions to manage, display, and analyze anomaly data. It not only tries to establish and unify data collection format in a ready to use format, but also intends to aid users in the creation of their own databases on their respective satellites for submission to NGDC for data archive and re-dissemination.

C. ANALYSIS

1. General

From the NGDC database, anomaly data from six satellites were selected for analysis by the Spacecraft Anomaly Manager (SAM) program for correlation of local time and seasonal dependencies on surface charging. SAM plots histograms of anomaly count by local time and by month to facilitate surface charging analysis. Histograms of reported anomalies by local time will plot only data reported with a local time while histograms of anomalies by month will plot all reported data for that family of satellites. The number of data points for these two histograms may not be the same because not all anomalies were reported with a local time.

Histograms of local time and seasonal anomaly occurrences can be used to determine spacecraft susceptibility to static charge buildup and subsequent discharge. Figure 17 shows histogram of SAM for all records in the NGDC database plotted against local time, and it illustrates the preponderance of midnight to dawn events. This is in agreement with the historical recognition that the local time distribution for anomalies peaks in the dawn sector, as shown in Figure 18 (McPherson et al., 1976). This local time dependence mirrors the local time

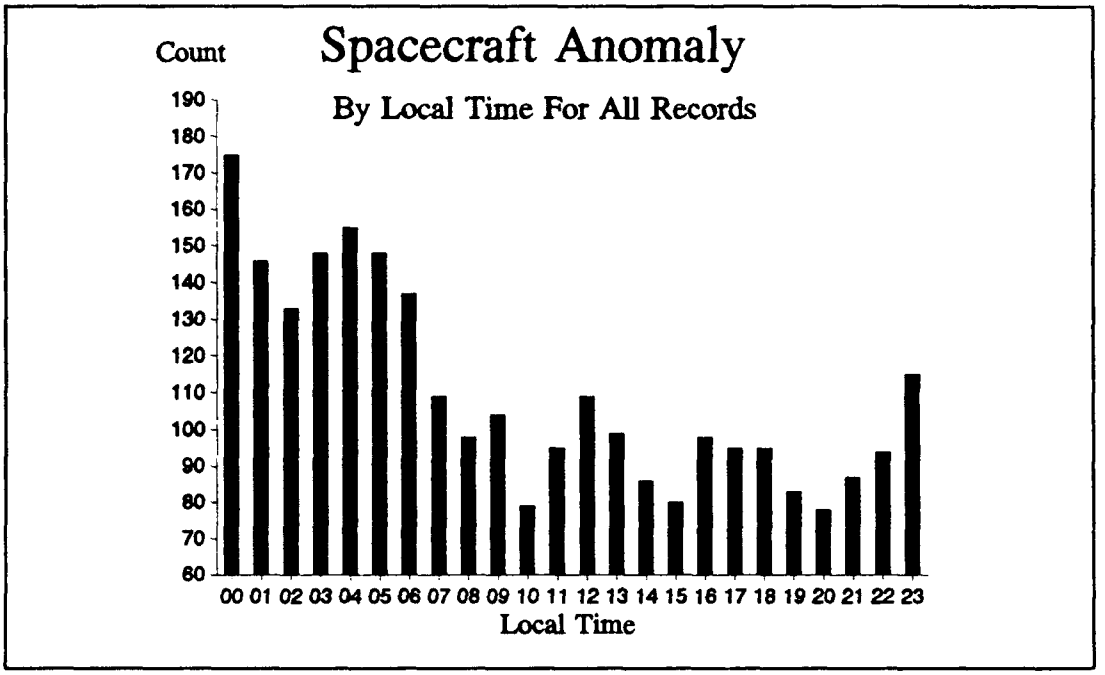

Figure 17. Local time distribution of all anomalies in the SAM database.

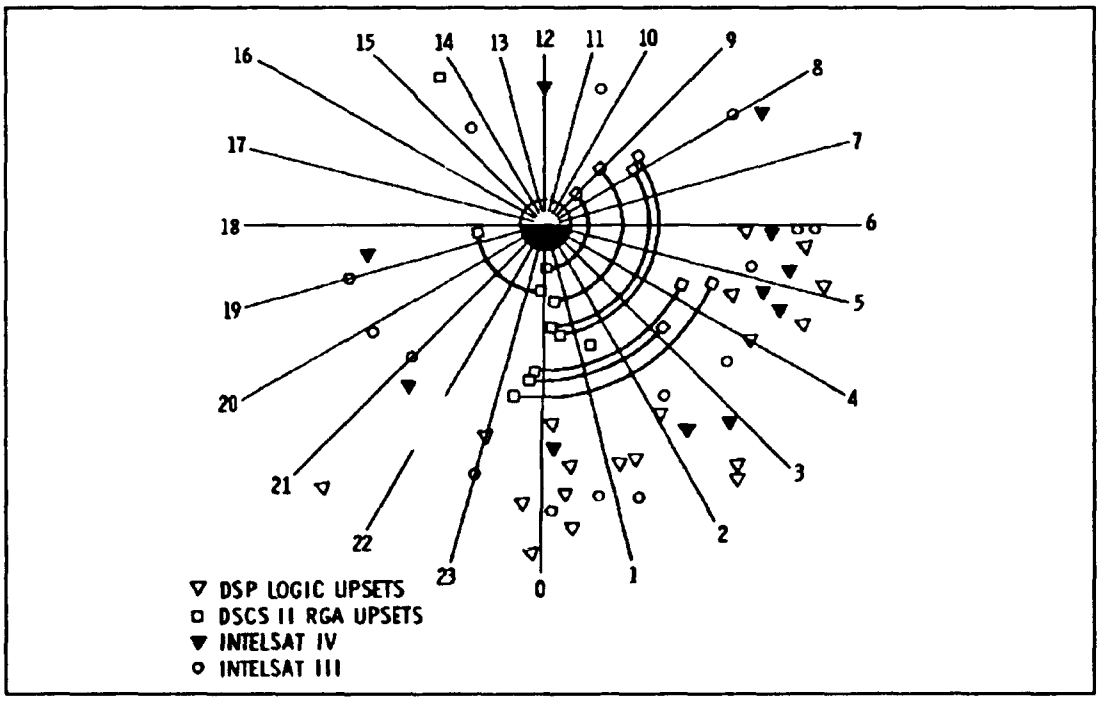

Figure 18. Local time dependence of circuit upset for several DoD and commercial satellites. (McPherson et al, 1976, Figure 1)

dependence for satellite charging at geosynchronous orbit, as found by Reasoner et al. (1976). Reasoner et al. analyzed 40 days of data from ATS-6 with the results that shown in Figure 19. Significant charging was found approximately 50 percent of the time at geosynchronous orbit in the midnight to dawn sector on ATS-6.

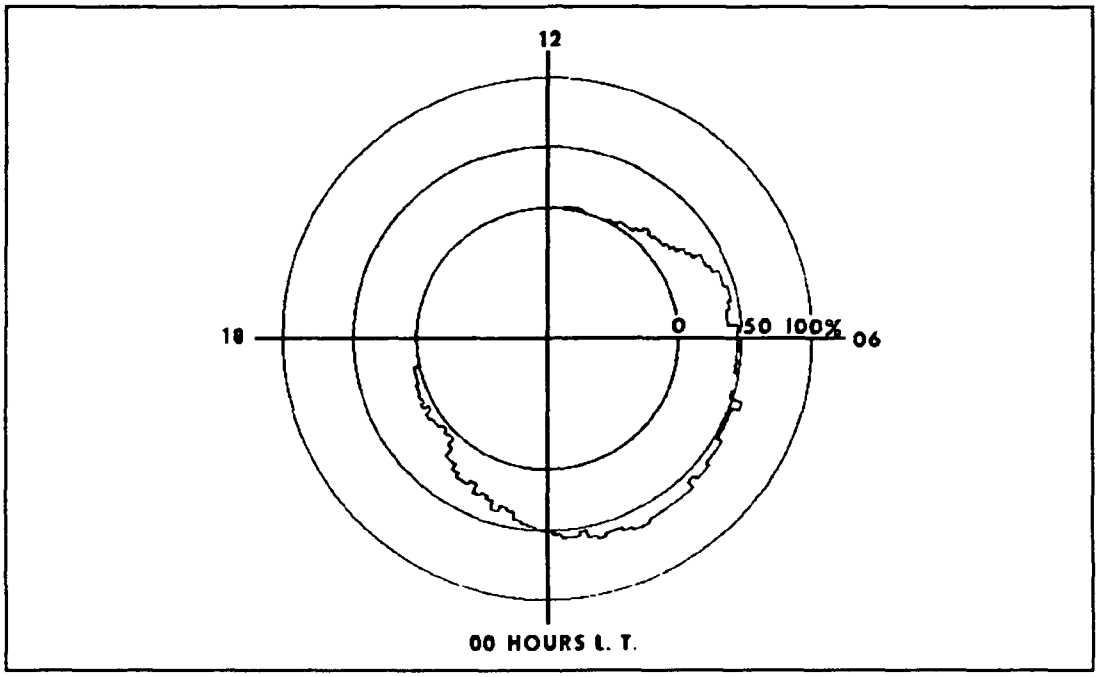

Figure 19. Local time distribution of ATS-6 spacecraft charging events. (Reasoner et al., 1976, Figure 7)

Figure 20 is a histogram of SAM for all anomaly records in the database plotted against month; it shows a curious increase during the equinox seasons. This pattern is not well known or fully understood. It will be found to be repeated in the consideration of individual satellites which follows.

2. Solar Cycle Correlation

The possible link between spacecraft anomalies and the 11 year solar cycle can also be considered using the NGDC database. The NGDC database provides

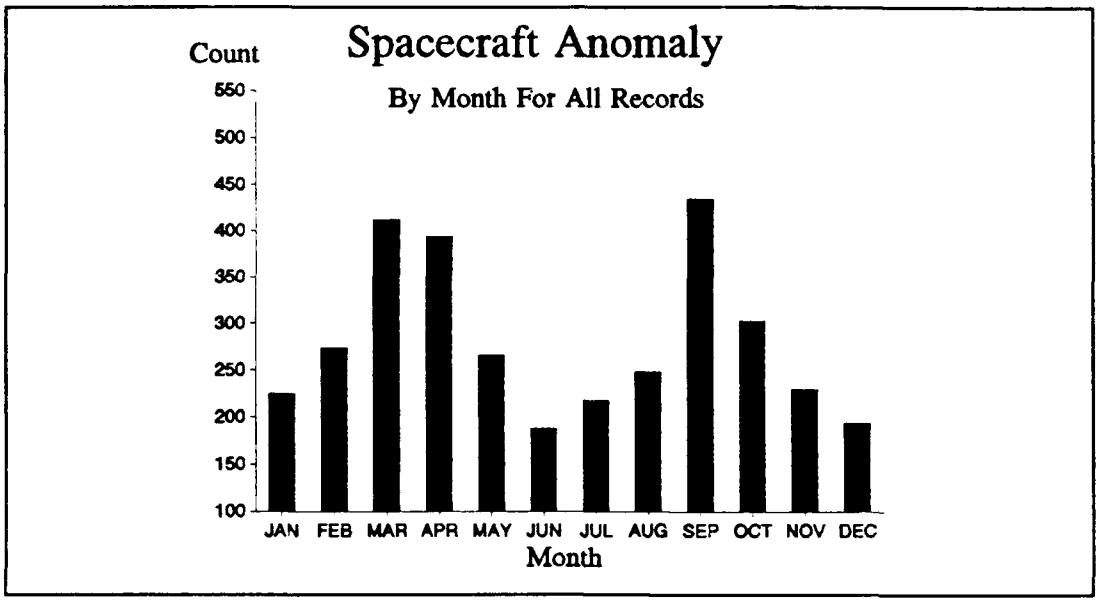

Figure 20. Monthly distribution of all anomalies in the SAM database.

a rough idea of how anomalies have varied over the last two solar cycles. There are some limitations:

- In the early seventies, the anomaly data collection was still in its infancy, and relatively few data points were gathered.
- As time went by, there were greater number of satellites on orbits that reported ytheir anomalies to the NGDC database.
- Data collection for this edition of the database was terminated after April 19, 1989, therefore, the anomaly counts in that year are not useful for the comparison.

Figure 21 plotted all reported anomalies of NGDC database versus year, and it shows two maxima. The first is at 1975, and the second is from 1983 to 1986. There is a minimum from 1977 to 1980. In Figure 21, there is a definite decrease of anomaly counts in two distinct periods. The first period is from 1977 to 1980, and

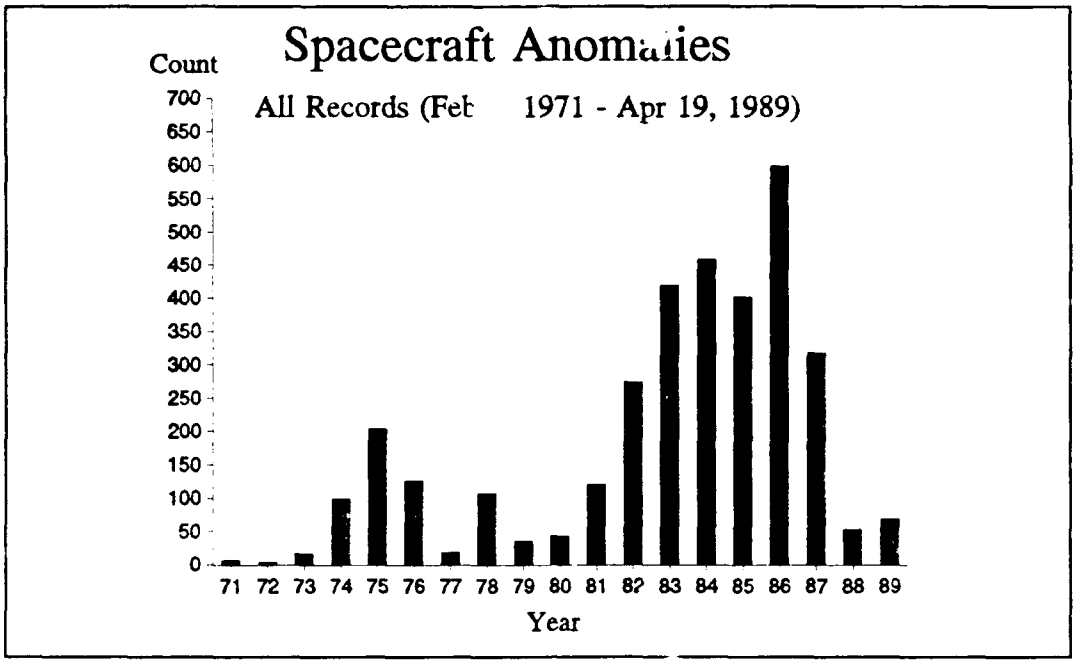

Figure 21. Anomaly counts per year in the SAM database.

the second period is at 1988. Figure 22 is a plot of the annual average sunspot numbers between 1971 to 1990. It shows two minima of solar minimum in 1976 and 1986. The anomaly occurrences in Figures 21 seem to be lagging behind the solar activities plotted in Figure 22. Careful comparison indicates a high degree of anti-correlation between anomalies and sunspot numbers. This is contrary to the trend we might expect, and needs to be reconsidered when the 1989-1990 anomaly records are updated.

This relationship is further pursued by considering one family of satellites. Anomaly data of the GOES satellite series were chosen. Figure 23 represents anomaly occurrences plotted by year for the respective variants of GOES. As mentioned earlier, data collected in 1989 only covered the first quarter of 1989.

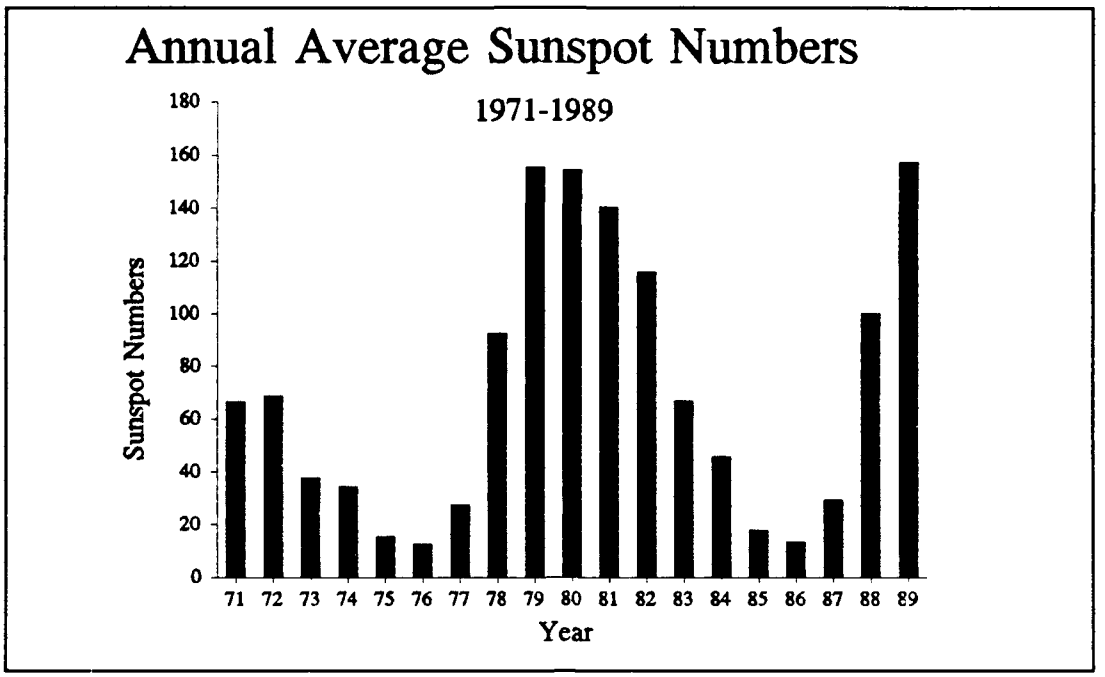

Figure 22. The annual average sunspot number from 1971 to 1989.

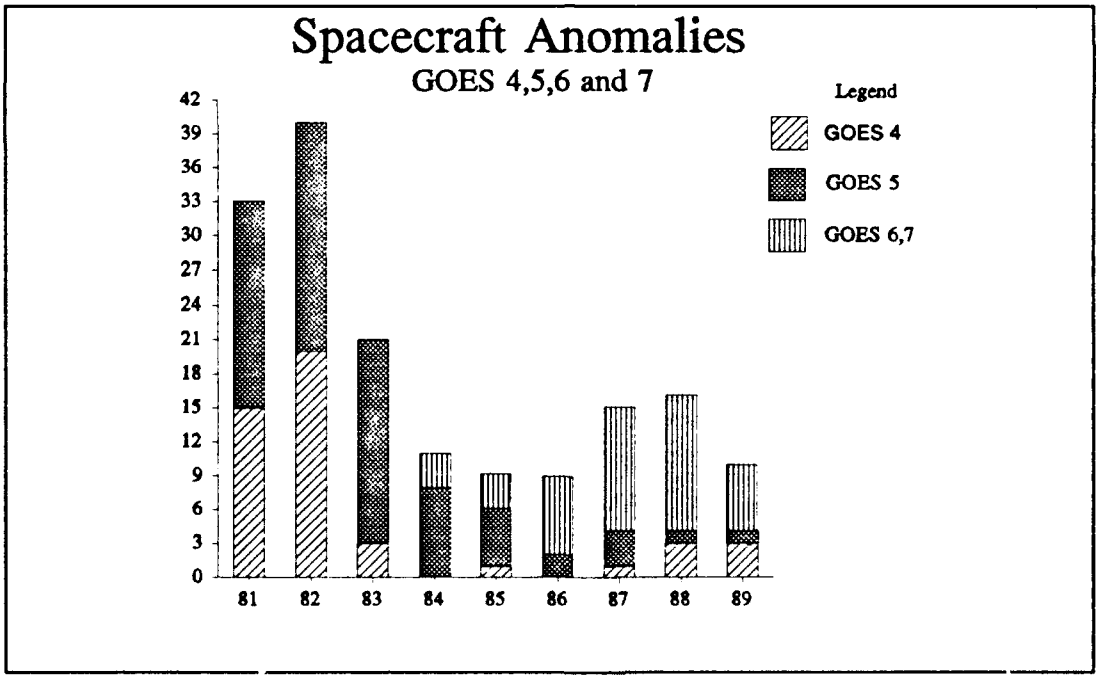

Figure 23. Anomaly counts of all variants of GOES satellites in the SAM database.

Furthermore, GOES-6 and -7 data were plotted together because there were so few of them. In Figure 23, GOES series satellite anomaly data show a minimum of anomaly occurrences at 1985 and 1986. Comparison of Figures 22, and 23 shows that the GOES anomaly distribution correlates to solar activity. This is in contrast to the results from the total database. This behavior should be reexamined when data are available from the high magnetic activity years -- 1990 and 1991.

3. Phantom Commands Due To Surface Charging

Anomalies associated with surface charging events are traditionally considered to occur from midnight to dawn. Reasoner et al. (1976), and McPherson et al. (1976) showed that phantom commands and satellite charging followed the same local time pattern as shown earlier in Figures 18, and 19. The initial plot of NGDC data (Figure 17) revealed that majority of anomalies occurred during that time period. This relationship was utilized in this study. Studies of the individual satellites will be focused on this same period. Histograms of anomaly counts by local time and month will be used to analyze ESD related anomalies for the midnight to dawn period and also for seasonal dependencies in surface charging. Histograms of anomaly count versus local time should show a relatively higher anomaly count concentrated in the period between midnight and 0600 hour if the anomalies are due to ESD's. For satellites at geosynchronous altitude, there are two periods of solar eclipse, each lasting 45 days centered around the vernal and autumnal equinoxes. The maximum period of eclipse in one day can last up to 1.2 hours. (Agrawal, 1986)

Histograms of anomaly count by month might show an increase of anomaly count in these two solar eclipse periods for surface charging related anomalies.

a. GOES

All reported anomalies of the GOES family in the NGDC database, a total of 144 anomalies for the period from March 1981 to April 1989, were plotted by local time and month in Figures 24 and 25 respectively. In Figure 24, by observing the plotted data available for the local time analysis, it is clear that from

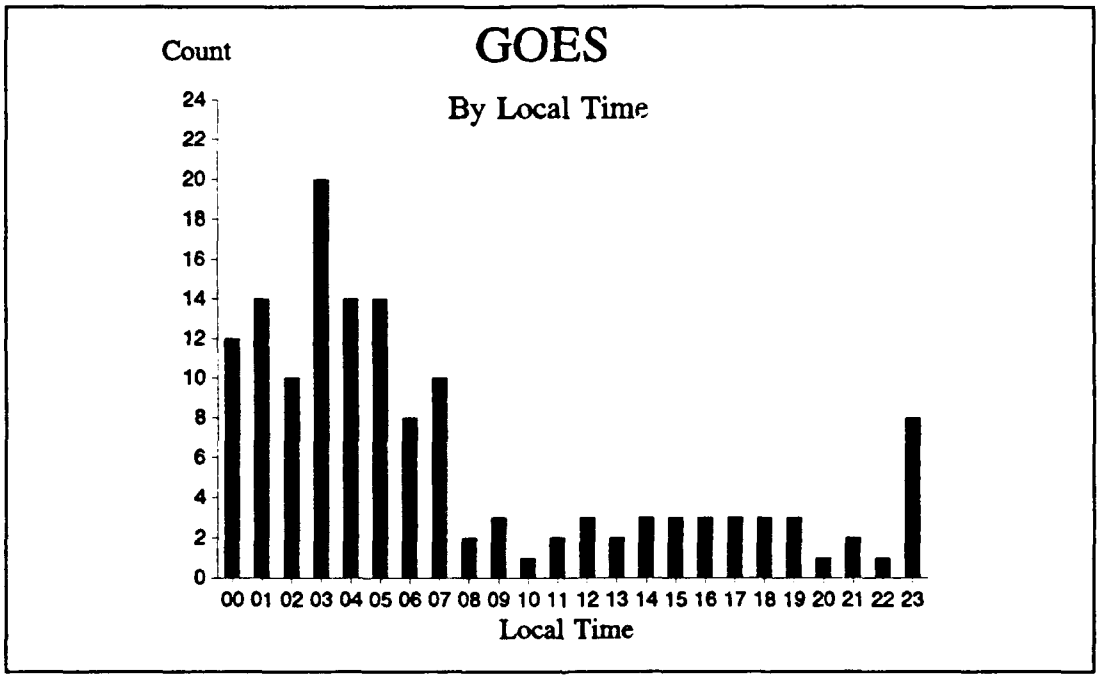

Figure 24. Local time distribution of all GOES anomalies.

midnight to 0700 there was a significantly higher occurrence of anomalies than for any other time of the day. Figure 25 shows that in the months of March/April (spring), and September/October (fall) anomaly counts were much higher than other

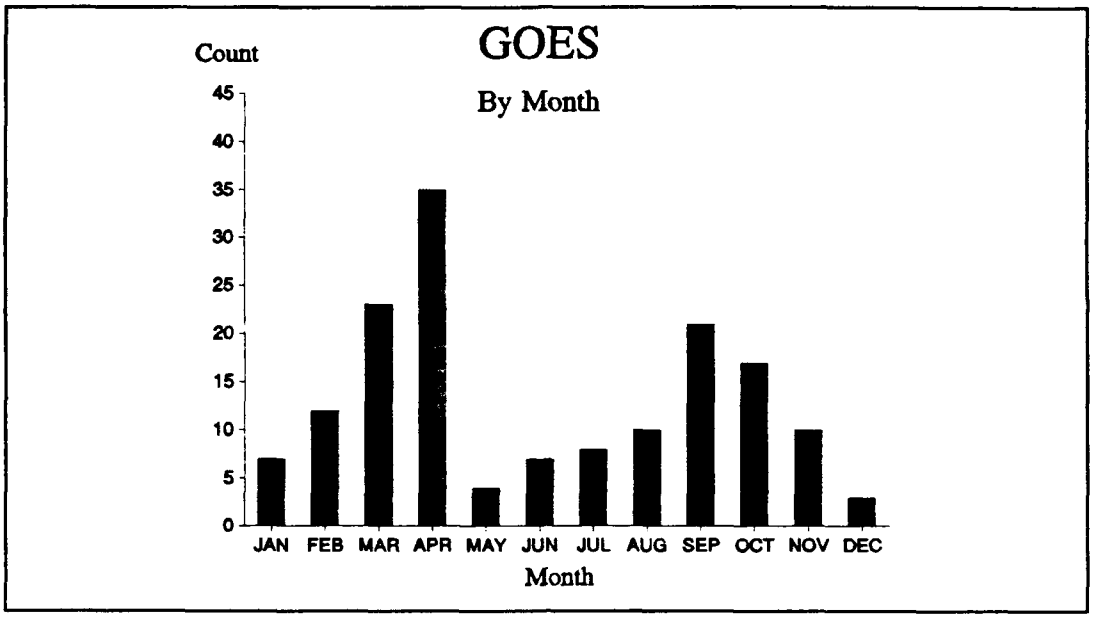

Figure 25. Monthly distribution of all GOES anomalies.

months. Further considerations of these areas of peak activity was done by plotting anomalies which occurred from between 0000 to 0700 local time of Figure 24 versus month in Figure 26. It is clear that the spring and fall seasons, March/April and September/October, have unusually high anomaly occurrences in the traditional midnight to dawn period. GOES family satellite anomalies exhibited the classic ESD patterns; reported GOES anomaly data clearly showed the midnight to dawn and seasonal dependencies. There is no obvious eclipse dependence (i.e., no increase at the 2300 or 0000 relative to 0200-0300 local time).

b. GG0

The next satellite considered here will be called GG0. The true identity of this satellite is confidential. Figure 27 is the histogram of anomalies by

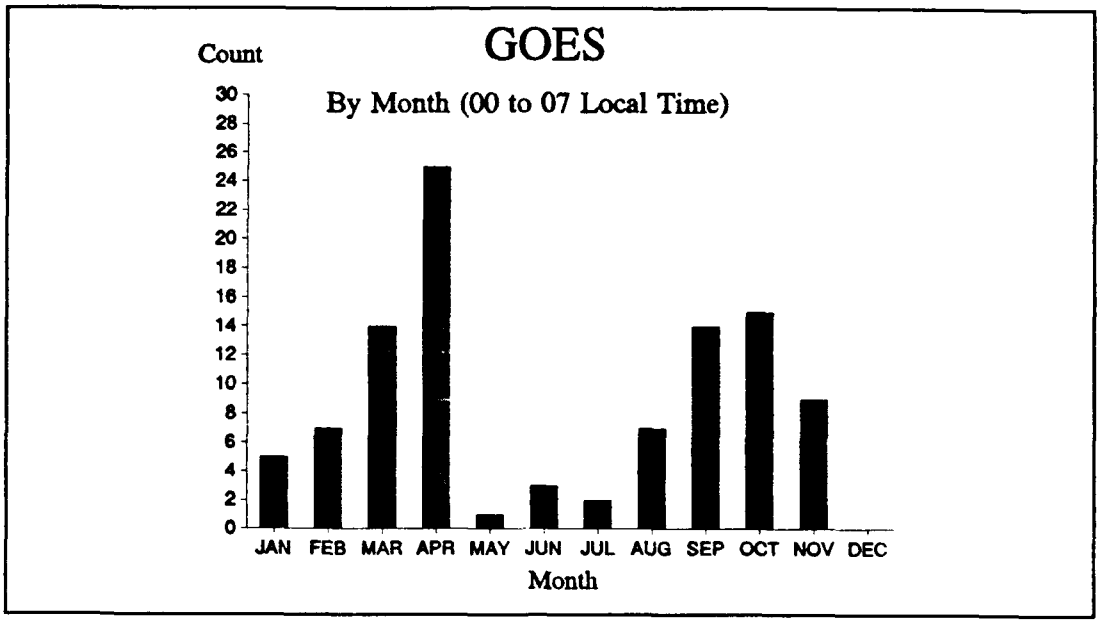

Figure 26. Monthly distribution of GOES anomalies between 0000 to 0700 hour local time.

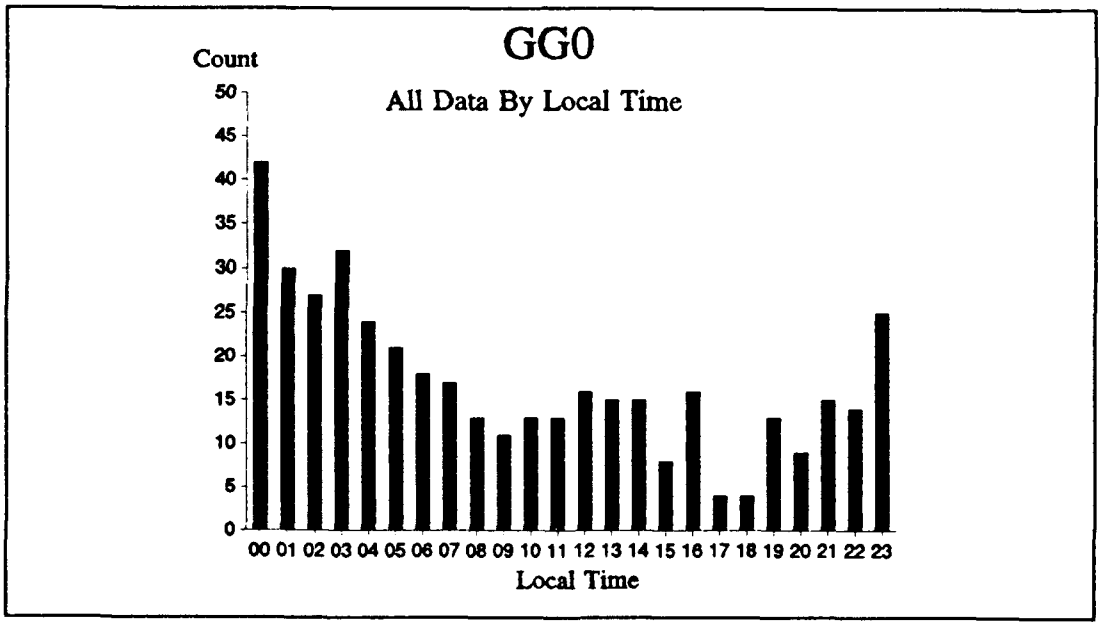

Figure 27. Local time distribution of all GG0 anomalies.

local time of GG0 which has 429 data points for the period from July 1973 to March 1989. There is a relatively high anomaly count occurring between 0000 and 0400 local time.

Figure 28 is a plot of the total GG0 satellite data by month which covers the period from February 1971 to March 1989. In this plot, the anomaly counts clearly shows a strong seasonal dependency, with peaks at April and October, corresponding to the vernal and autumnal equinox periods.

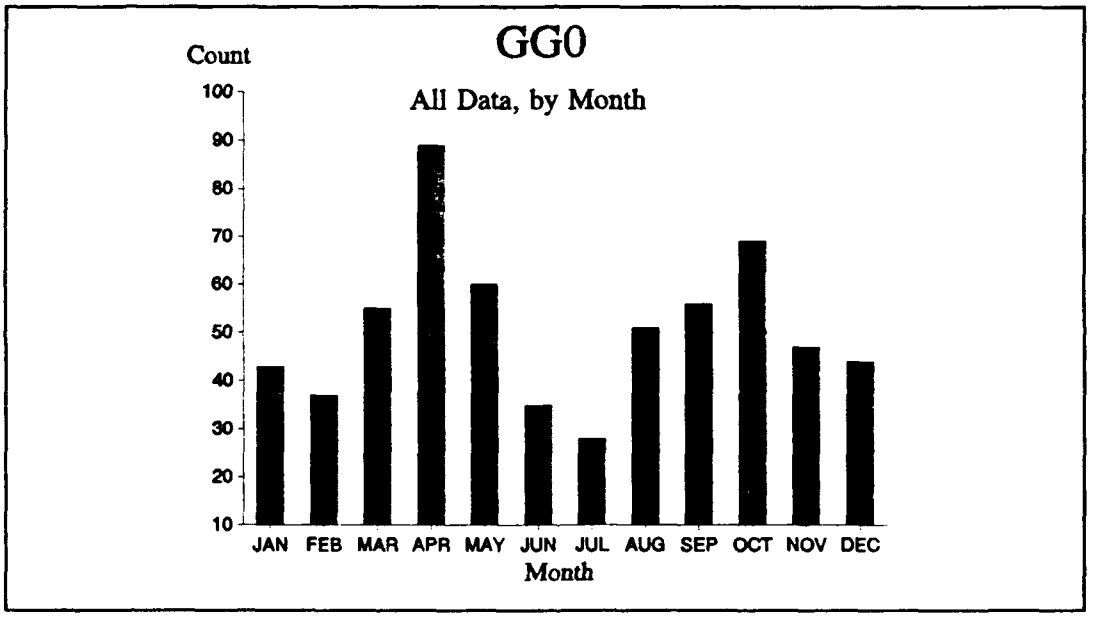

Figure 28. Monthly distribution of all GG0 anomalies.

Figure 29 is a histogram of the anomaly count plotted by month but restricted to anomalies from 0000 to 0700 local time. Figure 29 shows a much clearer seasonal dependence than in Figure 28. This indicates that GG0 anomalies

from 0000 to 0700 local time (traditional surface charging) have a stronger seasonal dependence than the set of anomalies which include effects such as SEU.

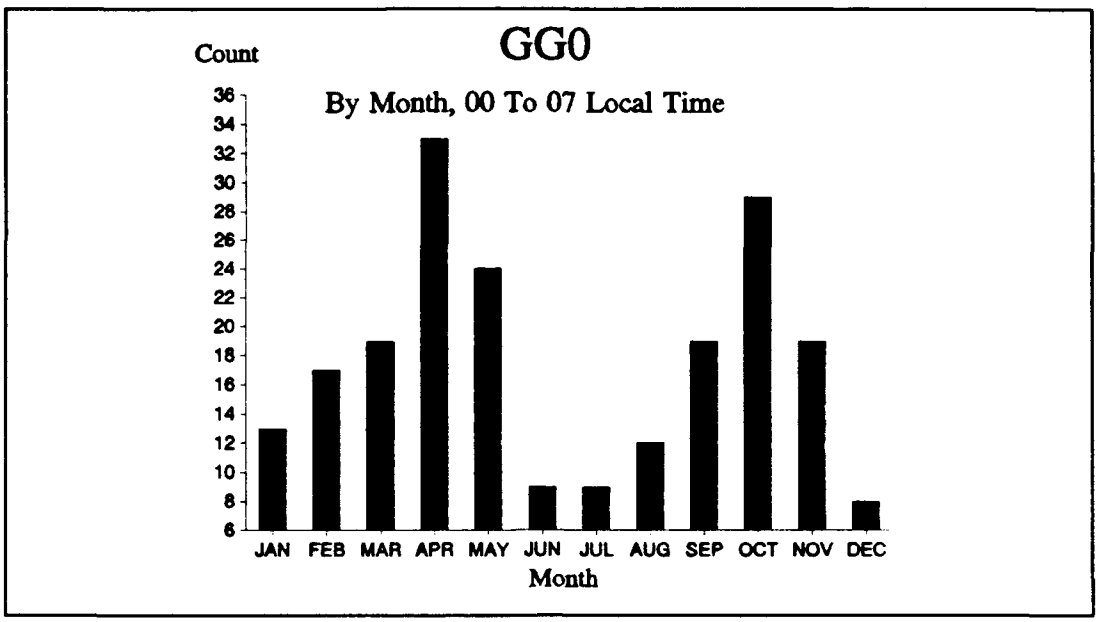

Figure 29. Monthly distribution of GG0 anomalies from 00 to 07 local time.

The nature of the seasonal dependence (Figures 28, 29), can be considered further. Figure 30 shows histograms of anomaly occurrences by local time for April and October data so that the midnight to dawn correlation of these two specific months can be examined. Figure 30 shows a midnight to dawn distribution. There are two other groups which are from 1000 to 1300, and from 2000 to 2300. They appear to be unrelated to the traditional association with surface charging.

c. GW0101

A second confidential satellite is identified as GW0101. GW0101 reported 294 anomalies between January 14, 1975 and November 26, 1976 (682 days).

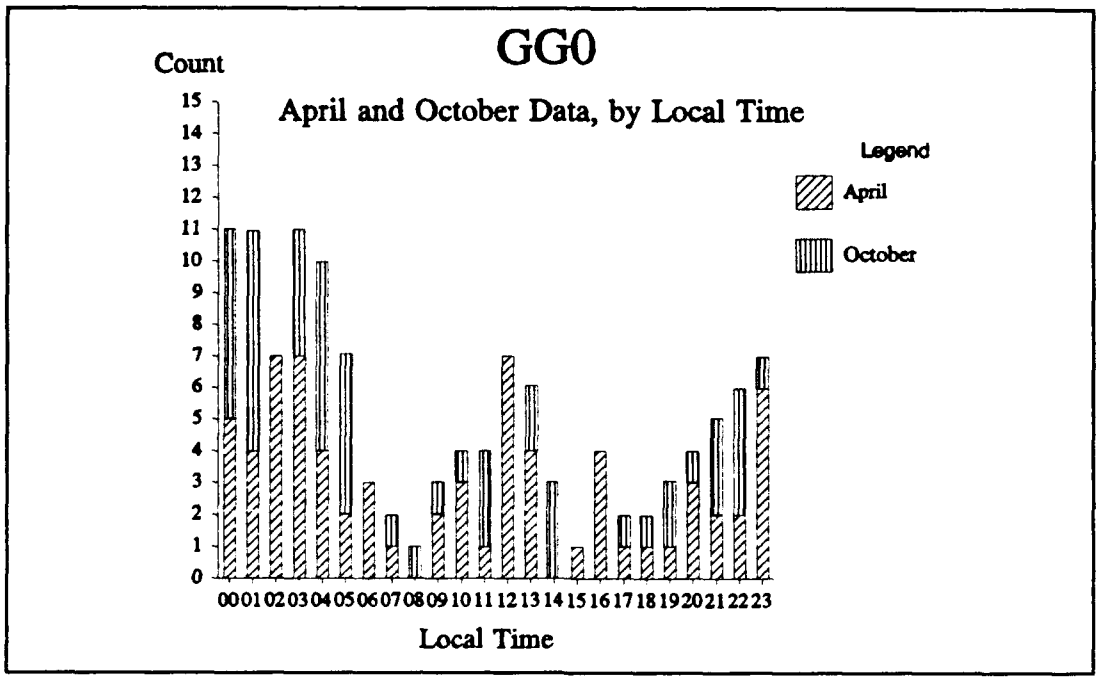

Figure 30. Local time distribution of GG0 anomalies for April and October.

Figure 31 is the histogram of the anomaly count by local time of the GW0101 data. There is a distribution of anomaly occurrences which indicates that there were anomaly causes other than surface charging, i.e., ECEMP. At 2000 local time, the anomaly count is high, which is abnormal for ESD induced anomalies.

A histogram of anomaly count versus month of GW0101 data is plotted in Figure 32. From this plot, anomaly counts in March and April were substantially higher than all other months; a much lower peak is centered on the fall equinox. GW0101 anomaly data show a very strong seasonal dependency, especially around spring equinox.

Figure 33 is a closer look of the March and April anomaly counts, plotted versus local time. A significant 61 percent of the total anomalies of 180 data

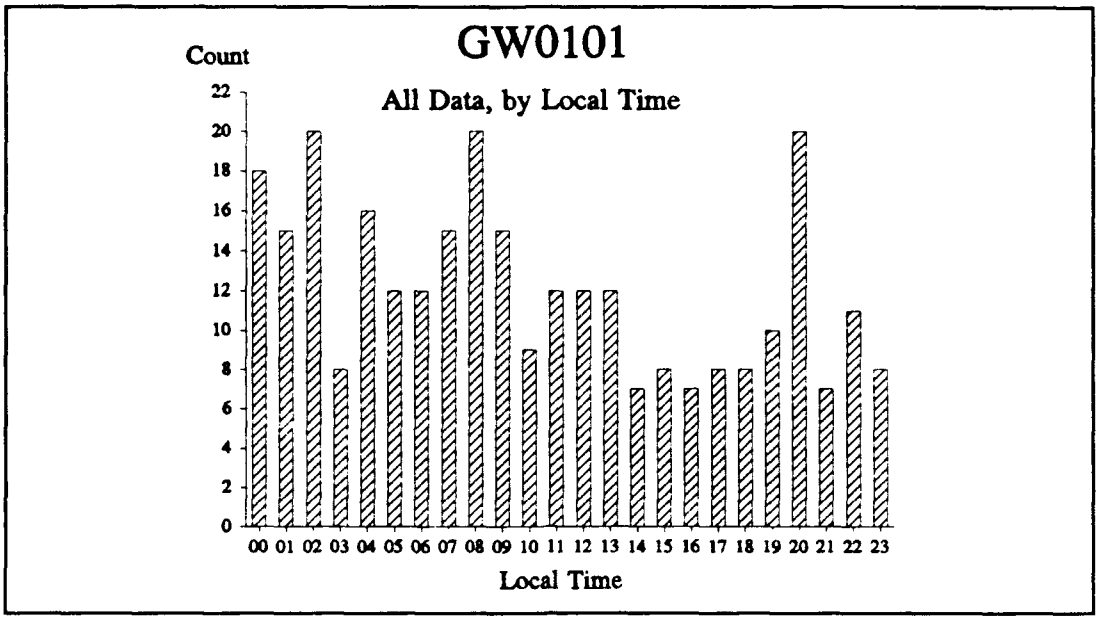

Figure 31. Local time distribution of all GW0101 anomalies.

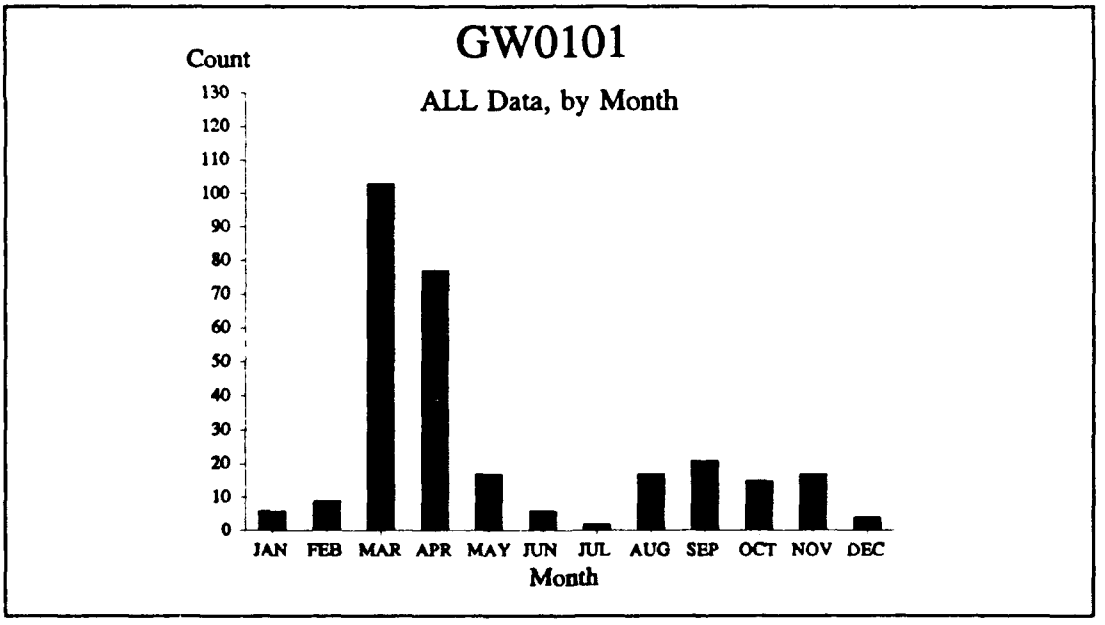

Figure 32. Monthly distribution of all Gw0101 anomalies.

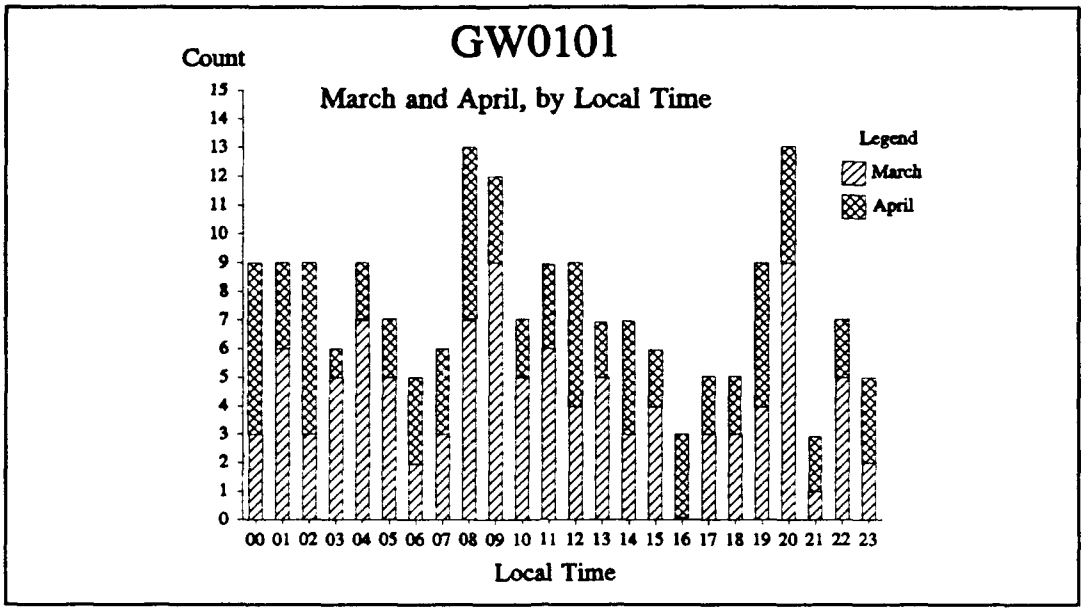

Figure 33. Local time distribution of March and April GW0101 anomalies.

points, occurred in these two months alone. Even by restricting the plots to the spring equinox, they do not produce the midnight to dawn distribution typically expected for ESD induced anomalies. These distributions suggest that environmentally induced anomalies other than ESD can have a strong seasonal dependence. Note that these anomalies were recorded during solar minimum (Figure 22). It appears that a large percentage of 1975-76 anomalies were from this satellite (see Figure 21).

d. METEOSAT

METEOSAT anomalies were described earlier in chapter two. A total of 193 METEOSAT anomalies, for METEOSAT -1 and -2, were reported for a 3458 day period between May 4, 1977 and October 22, 1986. Figure 34 is the

histogram of the anomaly count by local time of all METEOSAT data. There is a higher anomaly count period from 0300 to 0700 local time, and there appears to be an approximately three hour delay from the traditional midnight to dawn period. This delay was noted by Wrenn and Johnstone (1986).

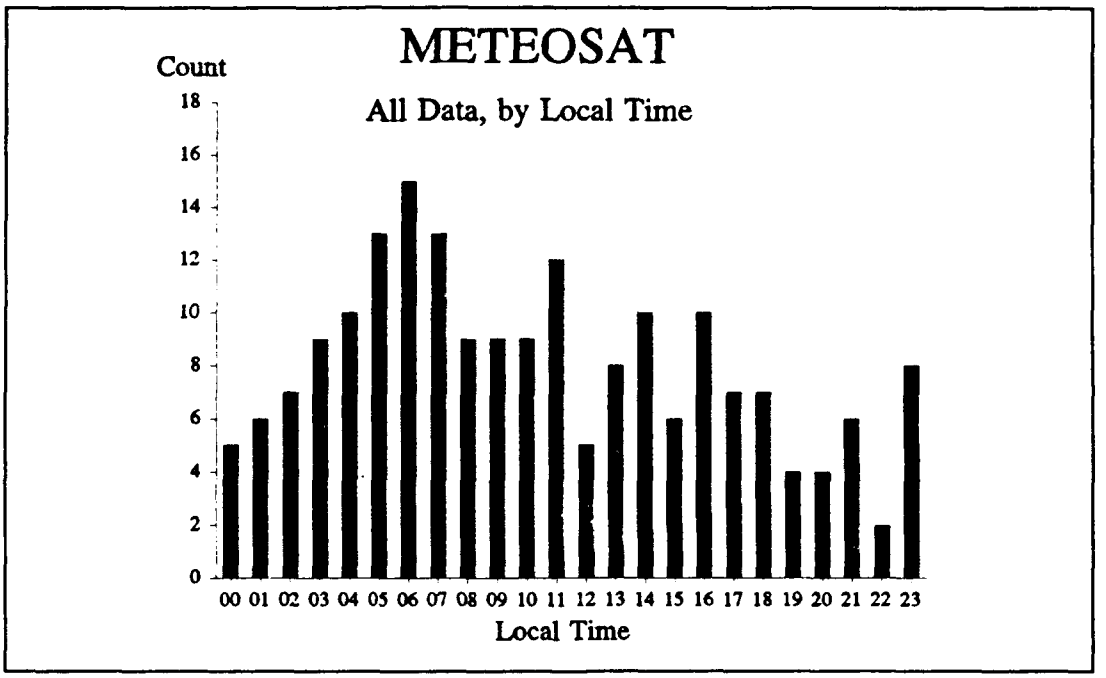

Figure 34. Local time distribution of all METEOSAT anomalies.

A histogram of anomaly count by month of all METEOSAT data is plotted in Figure 35. There are two maxima located at the spring and fall seasons and a third, an unusually high peak, in May. The spring and fall dependency was noted by Frezet et al. (1988); they found that the anomaly pattern followed the shadowing of the mirror assembly, indicating that this might be the cause. Hence, the seasonal effect may be due to shadowing patterns over the year for this satellite.

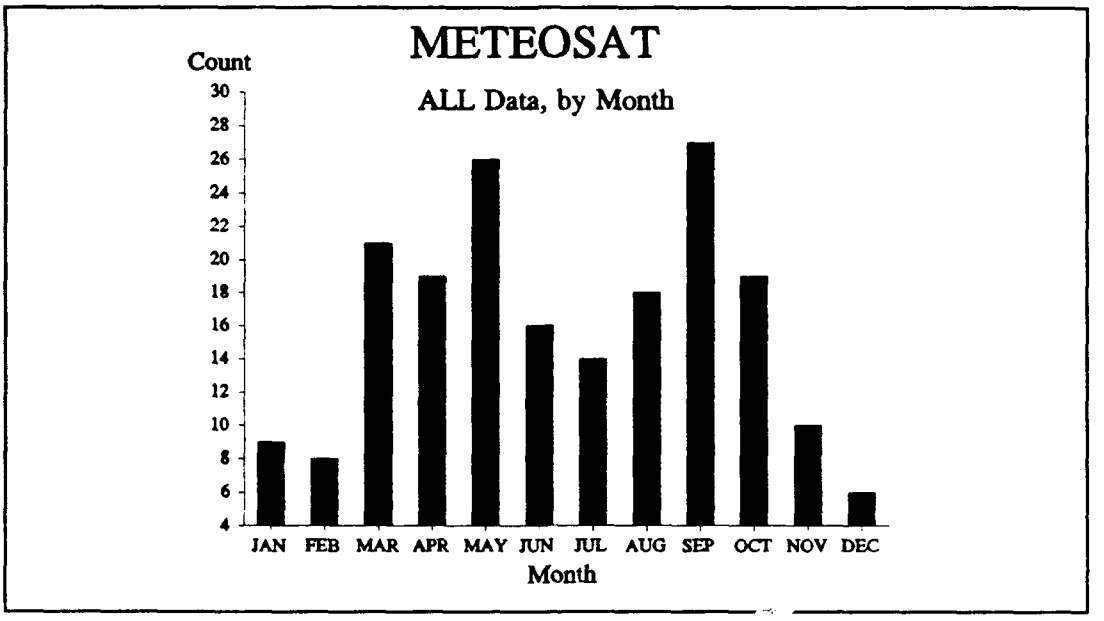

Figure 35. Monthly distribution of all METEOSAT anomalies.

Anomaly data for the period from 0300 to 0700 local time of Figure 34 were plotted by month in Figure 36 for seasonal correlation analysis. There are also two maxima in Figure 36 at March and September with May as the unexplained third peak. Anomaly data for the period between 1200 and 2300 local time of Figure 34 were also plotted by month in Figure 37 for further analysis. Two maxima exist at March and October.

Anomalies for March, April, September, and October in Figure 36 are plotted in histograms (anomaly count versus local time) as Figure 38 for the midnight to dawn analysis. Data in Figure 38 show a peak a 0600 local time. There four high anomaly periods which are at 0300/0700, 1000/1100, 1600/1800, and 2300 hours. Most anomalies occurred in the period from 0600 and 0800 hour. Data in Figure 38

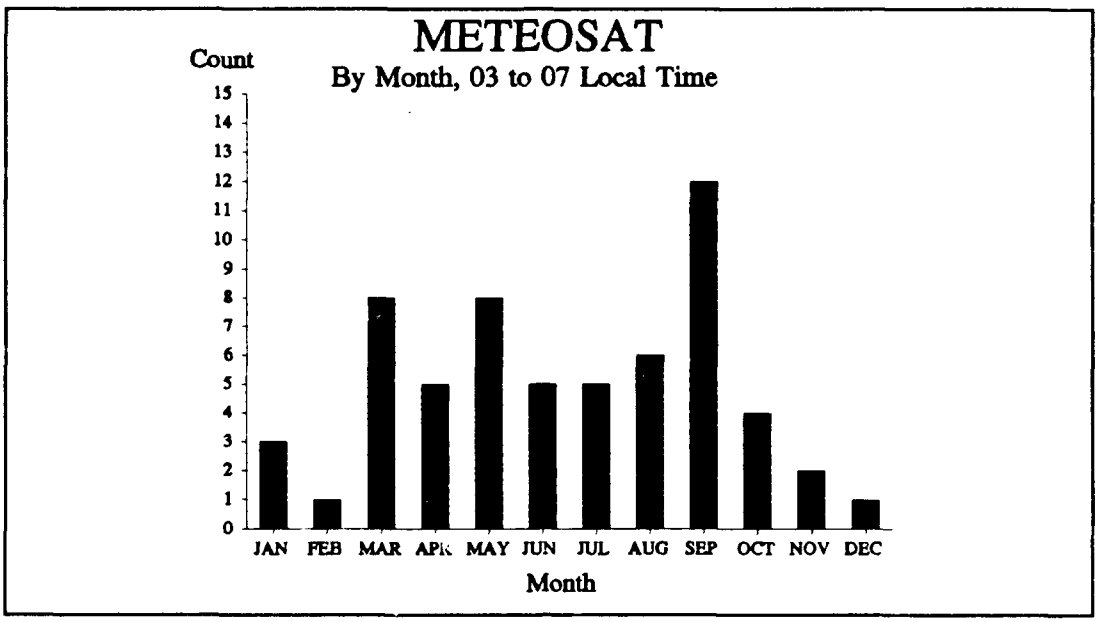

Figure 36. Monthly distribution of METEOSAT anomalies from 03 to 07 local time.

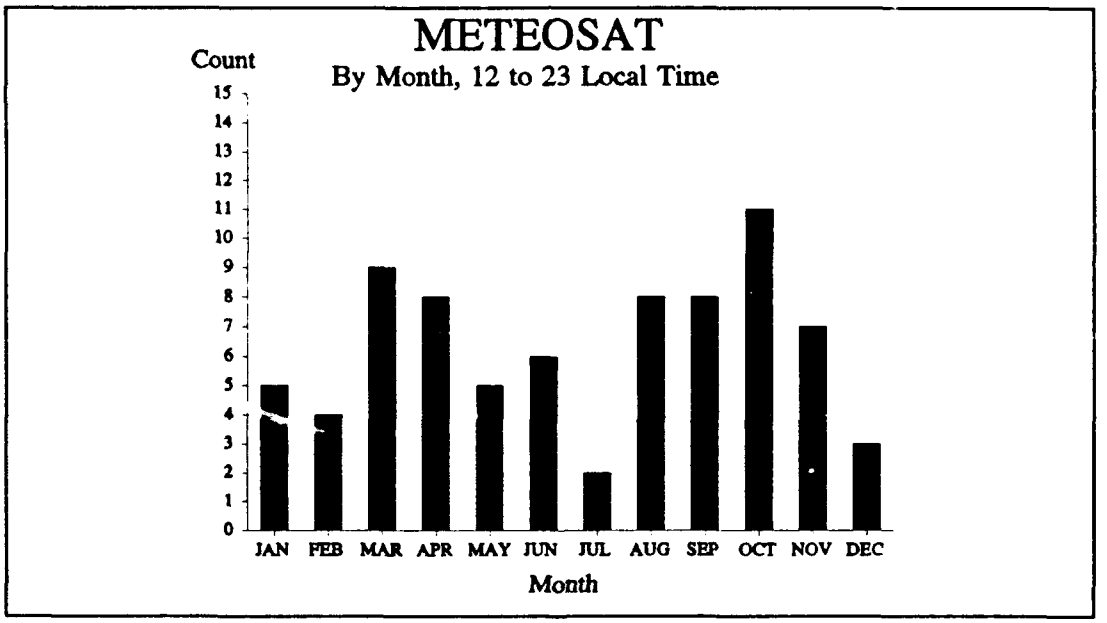

Figure 37. Monthly distribution of METEOSAT between 1200 to 2300 Local Time.

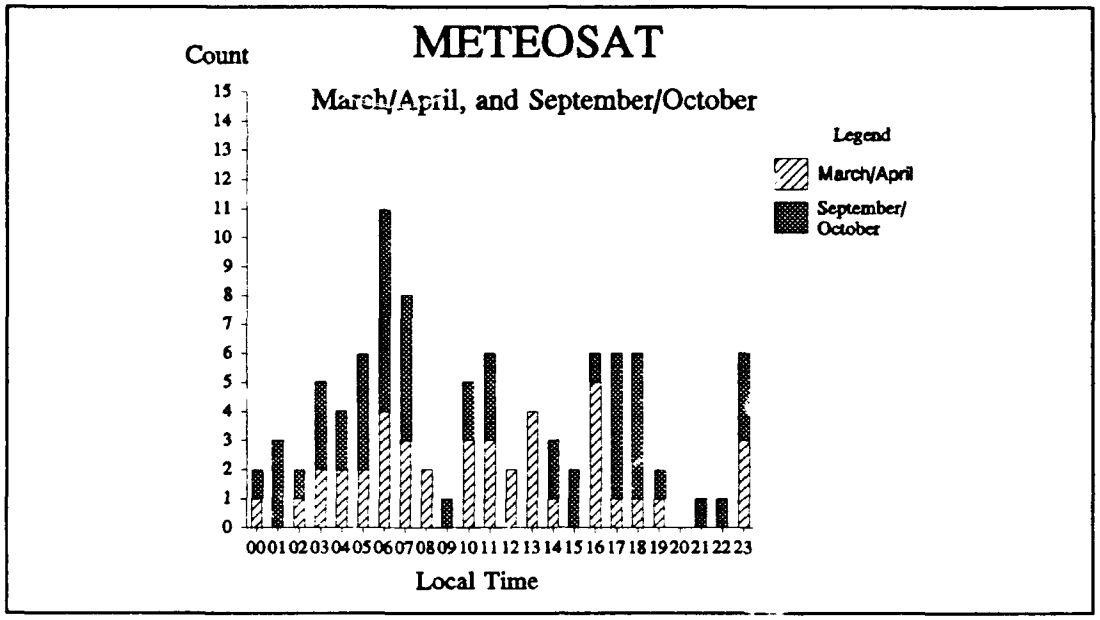

Figure 38. Local time distribution of March and April METEOSAT anomalies.

shows a midnight to dawn dependency; however, the anomalies were occurring with a three hour delay from the normally encountered local time distribution. Wrenn and Johnstone (1986) attributed this to the geometry of the satellite, and the shadowing patterns. In summary, METEOSAT data showed that its anomalies exhibited a seasonal dependence, and there were other causes of satellite anomalies beside ESD's illustrated by variations from the expected distributions in time and season. The seasonal dependence may have been due to shadowing of the mirror cavity.

e. DSCS

As introduced in page 23, the DSCS satellite system had many environmental problems. Figure 39 is the histogram of the DSCS anomalies by local time. DSCS satellites had a total of 128 reported anomalies, 125 of which were

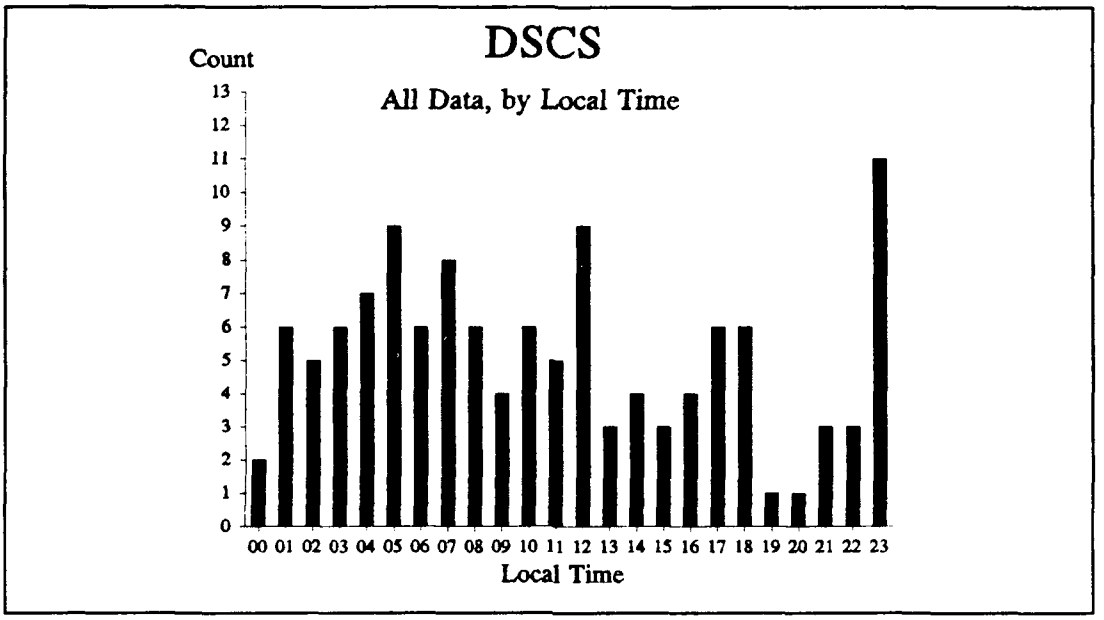

Figure 39. Local time distribution of all DSCS anomalies.

reported with the local time of the anomaly, for the period between December 22, 1973 and July 18, 1987. In Figure 39, there is evidence of a three hour delay of the midnight to dawn anomaly occurrences as with METEOSAT. Also, there is a significant peak at 2300 local time which may be eclipse related.

Figure 40 is the histogram of the anomaly counts by month for all DSCS anomalies. Anomalies mostly occurred on DSCS satellites in October through January. There are two distinct peaks at April and August, and a third large peak from October to January. The peak in April may be correlated to spring equinox as previously found, and the August may be associated with fall equinox. The third peak, from October through January, indicates that DSCS anomalies have a seasonal dependence which differs from the solstice/equinox pattern found for other satellites. This could be due to illumination patterns which also vary with seasons.

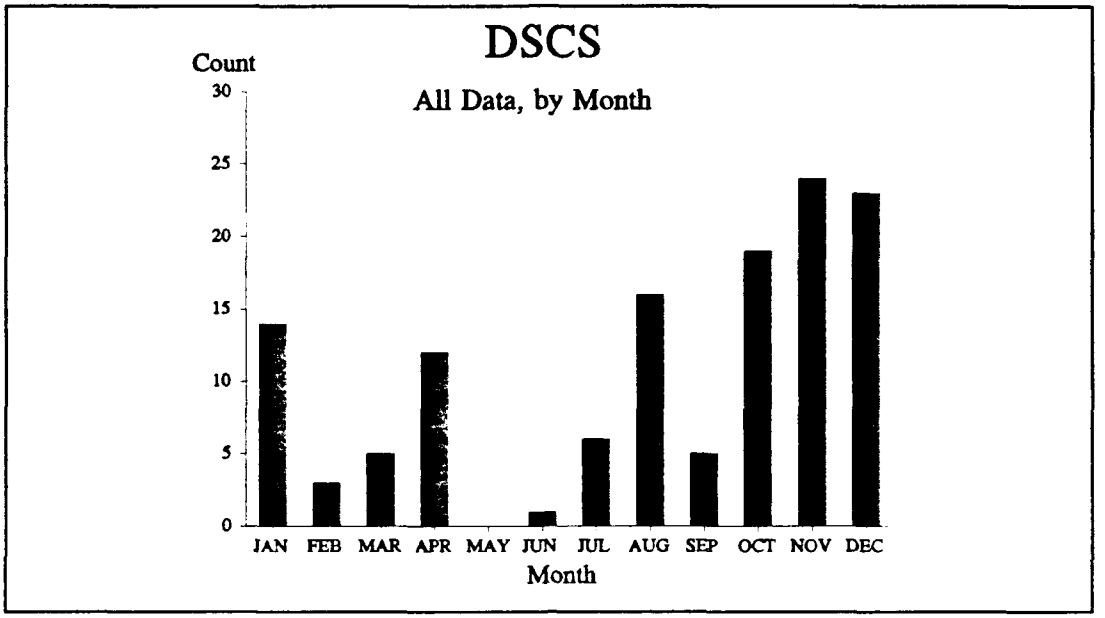

Figure 40. Monthly distribution of all DSCS anomalies.

f. GPS

GPS are semi-synchronous altitude (approximately 20,200 km) orbiting satellites. The operational constellation consists of 18 satellites in six orbital planes, and three satellites in each plane. The first GPS block one satellite was launched in 1978; the design of block two satellites started in 1982. Among the GPS data, 120 out of 564 total, only 23 percent had been reported with a local time between January 30, 1985 and July 17, 1987. Figure 41 is the histogram of the GPS anomalies by local time. There are three maxima of interest: 0000/0100, 0500/0600, and 1600 through 1900. The 0500/0600 peak is the highest of the three peaks. Seasonal analysis of these three maxima were plotted but not found to be useful due to insufficient data for the analysis.

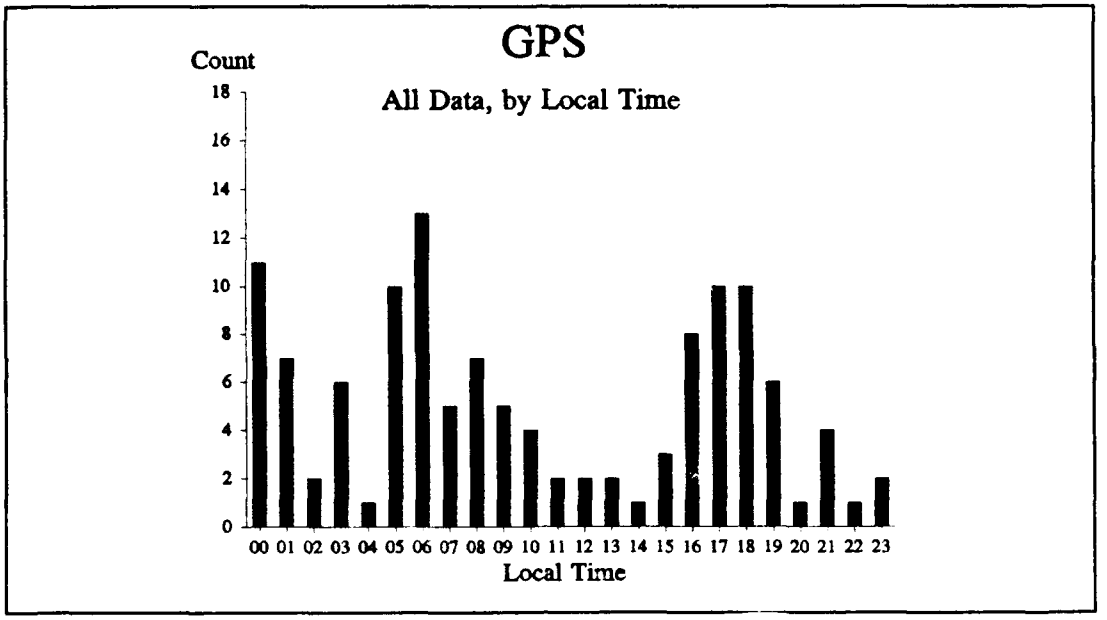

Figure 41. Local time distribution of all GPS anomalies.

Figure 42 shows all 564 reported GPS anomalies occurring between October 6, 1984 and August 18, 1987 in a 1046 day period. This data set is significantly larger than the one used for the midnight to dawn analysis in Figure 41 since local time was not available for all anomalies. There are two peak periods (January through February, and April through June) in Figure 42. Most of the anomalies occurred during the first half of the year, but March was unusually quiet. There are no obvious signs of seasonal dependency in this Figure. In general, the GPS anomalies (at semi-synchronous altitude) shows a different pattern compared to satellites at the geosynchronous altitude.

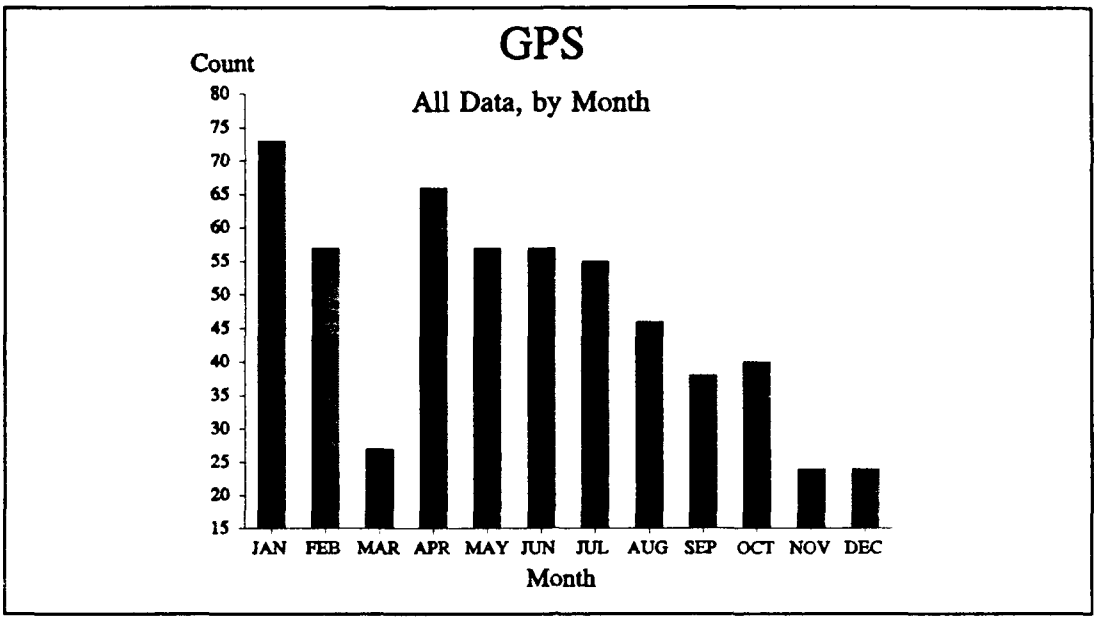

Figure 42. Monthly distribution of all GPS anomalies.

4. Surface Charging and GPS July 89 to March 90 Data

A survey of the anomaly logs for the GPS system was conducted for the nine month period from July 1990 to March 91. These logs were obtained from Captain Scardera of the 2nd Space Control Squadron, 2nd Space Wing Operations, U.S. Air Force Space Command. The 136 anomalies all had the appearance of SEU induced "soft errors", requiring that memory be reloaded. Figure 43 is a histogram of the anomaly count versus month for these GPS Block 2 anomalies. Unfortunately, the April, May, June of 1991 data were not available for the analysis, and Figure 43 was unable to present a full year data cycle. If there is a trend, it is a broad peak in the fall/winter. The anomaly counts for GPS, **semi-synchronous** orbiting satellites, demonstrated that most anomalies were caused by other anomaly producing mechanisms such as SEU's.

The anomaly count versus local time plot was not available since the anomaly data provided did not include local time information. However, it is recommended that the local time of the anomaly should be included in all future satellite anomaly reports so that these anomaly reports would be more useful for later analysis. It would also be useful if eclipse/sun conditions were noted.

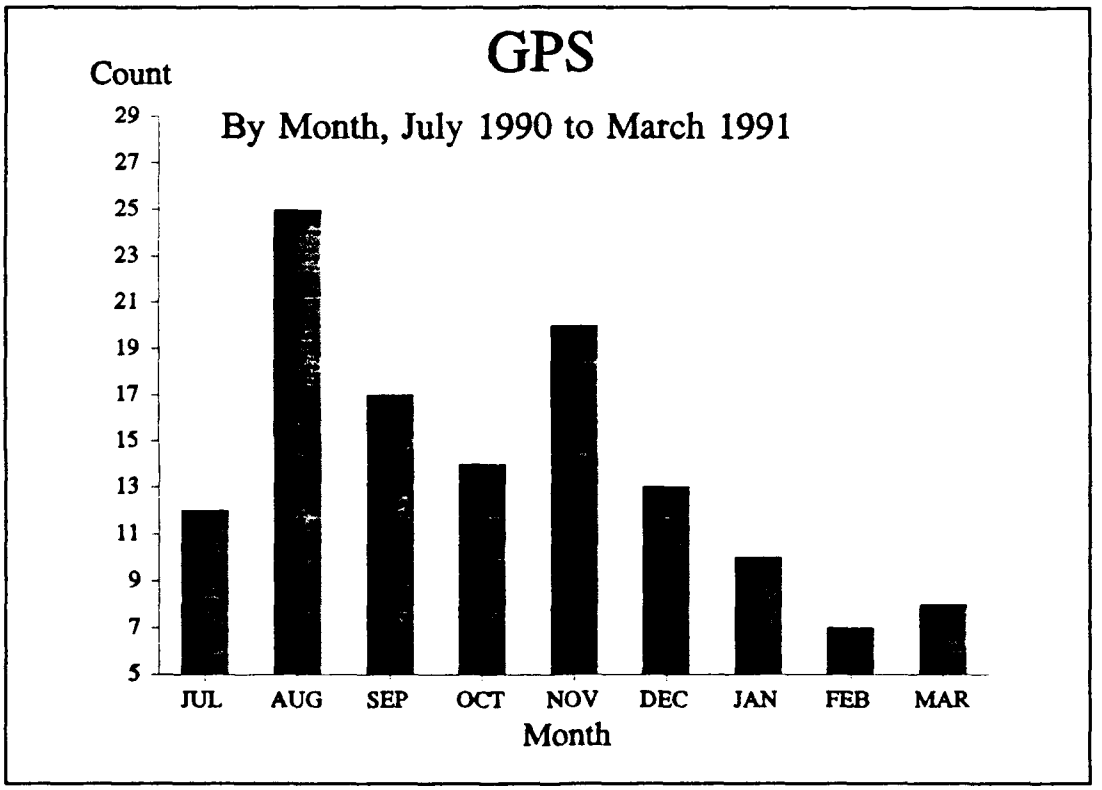

Figure 43. Monthly distribution of GPS anomalies from July 1990 to March 1991.

IV. SUMMARY AND CONCLUSIONS

A. SUMMARY

Various aspects of the space environment can cause on-orbit satellite anomalies. Studies have shown that adverse interactions between natural space environment and space systems can have deleterious consequences comparable to those caused by human or design errors. Electrostatic discharge (ESD), electron caused electromagnetic pulse (ECEMP), and single event upset (SEU) are the three most common anomaly producing mechanisms in space systems. The plasma environment, such as experienced in geosynchronous orbit, can cause differential charging of satellite components and lead to ESD on the surface of spacecraft. Anomalies attributable to ESD alone have been known to cause command errors, spurious signals, phantom commands, degraded sensor performance, part failure, and even complete mission loss. Numerous examples of ESD related anomalies have been given in section G of chapter two.

From the analysis, geosynchronous altitude satellites suffered anomalies have shown local time (midnight to dawn) and seasonal dependencies. Plotting anomaly data into histograms may be a viable method to analyze geosynchronous satellite anomalies in order to determine if the anomalies were ESD related. Once the cause of anomalies can be identified, then proper charge control measures can be included

in the future satellites designs. Hopefully, anomalies of the same cause would be eliminated.

By using the Spacecraft Anomaly Manager (SAM) software package, spacecraft anomaly data of operational satellites contained in the National Geophysical Data Center (NGDC) database were analyzed. Histograms of various anomaly data were plotted by year, local time, and month for solar cycle, local time (midnight to dawn), and seasonal dependencies.

Effects due to season may be related to the change in location of the earth's magnetic tail and the neutral sheet. During the equinox seasons, the satellite is in the center of the plasma sheet, while in the solstice seasons, the satellite may rise above or drop below the plasma sheet. (Nagai, 1987)

All NGDC reported anomalies were plotted by year in attempt to correlate spacecraft anomalies to the solar cycle; data in the NGDC database had shown a high degree of anti-correlation between spacecraft charging related anomalies and sun spot numbers. Anomaly data of GOES satellites were also plotted by year for the solar cycle correlation analysis. It was concluded that the GOES data exhibited a high degree of correlation between anomalies and the solar cycle.

Next, data in the NGDC database for six operational satellites were plotted in histograms, which displayed the anomaly count by local time or month. It was found that GOES family satellite anomalies showed a strong midnight to dawn and seasonal dependencies. The GOES histograms exhibited the classic anomaly distribution patterns which imply ESD causes. GG0 had 429 reported anomalies. Analysis

revealed that most of its anomalies were attributed to surface charging which were both local time (midnight to dawn) and seasonally dependent. Satellite GW0101 exhibits some midnight to dawn dependency and a strong seasonal dependency around March and April. For METEOSAT anomalies, histograms showed a four hour delay for the midnight to dawn dependence, the anomalies again showed a seasonal dependence. METEOSAT histograms suggested that surface charging was only one of the possible causes of anomalies. The DSCS anomalies showed a three hour delay from the normal midnight to dawn pattern, and also showed a different seasonal dependence than the other satellites. The NGDC's GPS anomaly data showed peaks at dawn, dusk, and midnight. No obvious seasonal dependence was found.

Finally, recent GPS anomalies obtained from the U.S. Air Force Space Command for the period between July 89 to March 90 were analyzed for seasonal dependency. The anomaly data (primarily SEU) showed a modest fall/winter enhancement.

B. CONCLUSIONS

From the anomaly analysis performed on the data of operational satellites contained in the NGDC database and recent GPS anomaly data from the U.S. Air Force Space Command, the following conclusions can be drawn:

- Anomaly occurrence patterns show peaks in the midnight-dawn region which imply they are caused by ESD induced by surface charging.

- Anomaly occurrences caused by ESD's are related to the solar cycle.
- ESD related anomalies are local time dependent with peaks in the equinox seasons.
- ESD related anomalies are seasonal dependent.
- Histograms are an effective manner to display anomaly occurrences for both local time and seasonal dependency analysis.
- SAM is an useful analytical tool which can quickly determine an anomaly data set if the anomalies are related to the surface charging mechanism.

C. RECOMMENDATIONS

From the result of the anomaly analysis, an active charge control requirement for future DoD geosynchronous satellites is recommended as follows:

- Proper engineering solutions should be integrated into satellite designs to prevent ESD from causing anomalies. This can be done effectively on multi-satellite programs such as GPS.
- Active charge control is recommended for all DoD satellites which cannot tolerate functional anomalies due to ESD's, and on the first flight of all new satellite designs. Active charge control devices, such as a plasma emitter, can consistently maintain the desired spacecraft surface potential (Olsen, 1981).
- Passive charge control measures, such as thicker shielding and electrostatic cleanliness, are recommended to be integrated into all satellite designs. Passive charge control measures showed general success in all applications (Olsen et al., 1988).

Additionally, it is recommended that the Air Force Space Command should include local time, location, and sun/eclipse information of satellites when submitting anomaly reports on GPS to the National Geophysical Data Center (NGDC) in Boulder, Colorado.

LIST OF REFERENCES

Agrawal, B.N., *Design of Geosynchronous Spacecraft*, pp. 323, Prentice-Hall, Inc., 1986.

Allen, J.H., *Solar and Geomagnetic Activity During March 1989 and Later Months and Their Consequences at Earth and in Near-Earth Space*, Proceedings of the Spacecraft Charging Technology Conference, Olsen, R.C., Editors, pp. 24, Naval Post Graduate School, Monterey, CA, January 1991.

Binder, D., Smith, E.C., and Holman, A.B., "Satellite Anomalies from Galactic Cosmic," *IEEE Transaction on Nuclear Science*, Vol. NS-29, pp. 2085, 1982.

DeForest, S.E., "Spacecraft Charging at Synchronous Orbit," *Journal of Geophysical Research*, Vol. 77, No. 4, pp. 651-659, February 1977.

Frezet, M., Granger, J.P., Levy, L., and Hamelin, J., "Assessment of Charging Behavior of Meteosat Satellite in Geosynchronous Environment," *IEEE Transactions on Nuclear Science*, Vol. 35, No. 6, pp. 1400-1406, December 1988.

Frooninckx, T., and Sojka, J.J., "Solar Cycle Dependence of Spacecraft Charging in LEO," paper submitted to Journal of Geophysical Research, March, 1991.

Hoge, D.G., "Results of Meteosat-F2 Spacecraft Charging Monitors," *Proceedings of an International Symposium on Spacecraft Materials in Space Environment*, pp. 175, France, June 8-12, 1982.

Johnstone, A.D., Wren, G.L., Huckle, H.E., and R.F. Scott, "Meteosat F2 spacecraft charging monitors," *Final Report ESA*, Contracts 4715/81/F/CG and 5911/84/F/CG, November, 1985.

Koons H.C. and Gorney D.J., *Spacecraft Environmental Anomalies Except System: A Status Report*, Aerospace Report No. ATR-88(9562)-1, pp. 54, 1 December, 1988.

Koons, H.C., Mizera, P.F., Roeder, J.L., and Fennell, J.F., "Severe Spacecraft-Charging Event on SCATHA in September 1982," *Journal of Spacecraft and Rockets*, Vol. 25, No. 3, pp. 239-243, May-June 1988.

Lancaster, "Solar Activity Could Disrupt Communications," *Aviation Week & Space Technology*, Vol.134, No.3, pp. 63, January 21, 1991.

Lechte, H.G., "Electrostatic Immunity of Geostationary Satellites," *Advisory Grou for Aerospace Research & Development Conference Proceedings No. 406*, pp. 24-2,3, Netherlands, June 2-6, 1986.

Lechte, H.G., *Space Environment Technology*, pp. 653, Cepadues-Editions, 1987.

Leung, P., Whittlesey, H.B., Robinson Jr, P.A., "Environment-Induced Electrostatic Discharges as the Cause of Voyager 1 Power-On Resets," *Journal of Spacecraft and Rockets*, Vol.23, No.3, pp. 323-330, May-June 1986.

McPherson, D. A. and Schober W.R., " Spacecraft Charging At High Altitudes: The SCATHA Satellite Program," *Spacecraft Charging by Magnetospheric Plasmas, Progress in Astronautics and Aeronautics,* Vol. 47, pp. 15-30, MIT Press, Cambridge, MA, 1976.

Meulenberg Jr, H., "Evidence for a New Mechanism for Dielectrics in a Plasma," *Spacecraft Charging by Magnetospheric Plasmas, Progress in Astronautics and Aeronautics,* Vol. 47, pp. 237-246, MIT Press, Cambridge, MA, 1976.

Nagai, T., "Interplanetary Magnetic Field B_y Effects on the Magnetic Field at Synchronous Orbit," *Journal of Geophysical Research*, Vol. 92, No. A10, pp. 11,215-11,220, October 1, 1987.

Olsen, R.C., "Modification of Spacecraft Potentials," *Journal of Spacecraft and Rockets*, Vol.18, No. 5, pp.462-469, September-October 1981.

Olsen, R.C., McIlwain, C.E., and Whipple, E.C., "Observations of Differential Charging Effects on ATS 6," *Journal of Geophysical Research*, Vol. 86, No. A8, pp. 6809-6819, August 1, 1981.

Olsen, R.C. and Whipple, E.C., "An Unusual Charging Event on ISEE 1," *Journal of Geophysical Research*, Vol. 93, No. A6, pp. 5568-5578, June 1, 1988.

Reagan, J.B., Nightingale, R.W., Gaines, E.E., Meyerott, R.E., and Imhof, W.L., "Role of Energetic Particles in Charging/Discharging of Spacecraft Dielectrics," *Spacecraft Charging Technology 1980,* NASA-CP-2182, Air Force Geophysics Lab., TR-81-0270, pp.74-85, 1981.

Reasoner, D. L., Lennartsson, D.L., and Chappell, C. R., " Relationship Between ATS-6 Spacecraft-Charging Occurrences and Warm Plasma Encounters," *Spacecraft Charging by Magnetospheric Plasmas, Progress in Astronautics and Aeronautics,* Vol. 47, pp. 89-101, MIT Press, Cambridge, MA, 1976.

Robbins, A., "Meteosat Spacecraft Charging Investigations," *Final Report ESA*, Contract 3561/78F/GG/SC, 1979.

Robinson Jr., P.A., *Spacecraft Environmental Anomalies Handbook*, Geophysics Laboratory, GL-TR-89-0222, 1989.

Rosen, A., "Spacecraft Charging: Environment-induced anomalies," *Journal of Spacecraft and Rockets*, Vol.13, pp.129, 1976.

Shane, D.F., *Spacecraft Charging Technology Conference, P78-2*, AFGL TR-77-0051, Proceedings of the Spacecraft Charging Technology Conference, Pike, C.P. and Lovell, R.R., Editors, pp.23-25, AFGL, Hanscom AFB, MA, 1977.

Shaw, R.R., Navevicz, J.E., and Adamo, R.C., "Observations of Electrical Discharges Caused by Differential Satellite-Charging," *Spacecraft Charging by Magnetospheric Plasmas, Progress in Astronautics and Aeronautics*, Vol. 47, pp. 61-76, MIT Press, Cambridge, MA, 1976.

Stevens, N.J. and Klinect, V.W., "Summary of the CTS Transient Event Count Data After One Year of Operation," NASA TM 73710, paper presented at the Nuclear and Space Radiation Effects Conference, Williamsburg, VA July 12-15, 1977.

Vampola, A.L., "Thick Dielectric Charging on High-Altitude Spacecraft," *Journal of Electrostatics*, Vol.20, pp. 21-30, 1987.

Wadham, P.N., "The Effects of Electrostatic Discharge Phenomena on Telesat's Domestic Communications Satellites," *Advisory Group for Aerospace Research & Development Conference Proceedings No. 406*, pp. 25-3,4, Netherlands, June 2-6, 1986.

Wrenn, G.L. and Johnstone, "Spacecraft Charging: Meteosat experience," *Advisory Group for Aerospace Research & Development Conference Proceedings No. 406*, pp. 25-1, Netherlands, June 2-6, 1986.

Whipple, E.C., *The Equilibrium Electric Potential of a Body in the Upper Atmosphere*, NASA Report X-615-65-296, 1965.

Telephone conversation between Dr. Harry Koons of Aerospace Corporation and the author, May 28, 1991.

Telephone conversation between Captain Mike Scardera, 2nd Space Control Squadron, 2nd Space Wing Operations, USAF and the author, 4 April 1991.

INITIAL DISTRIBUTION LIST

1.	Defense Technical Information Center Cameron Station Alexandria, VA 22304-6145	2
2.	Library, Code 52 Naval Postgraduate School Monterey, CA 93943-5002	2
3.	Commandant of the Marine Corps Code TE 06 Headquarters, U.S. Marine Corps Washington, D.C. 20380-0001	1
4.	Chairman, Space Systems Academic Group, Code 72 Naval Postgraduate School Monterey, CA 93943-5000	1
5.	Dr. R. C. Olsen, Code PH/OS Department of Physics Naval Postgraduate School Monterey, CA 93943-5002	20
6.	Dr. J. L. Roeder M2/260 Aerospace Corporation P.O. Box 92957 Los Angeles, CA 90009	1
7.	Dr. D. J. Gorney M2/260 Aerospace Corporation P.O. Box 92957 Los Angeles, CA 90009	1

8. Dr. H. C. Koons — 1
M2/260
Aerospace Corporation
P.O. Box 92957
Los Angeles, CA 90009

9. Dr. J. Fennel — 1
M2/259
Aerospace Corporation
P.O. Box 92957
Los Angeles, CA 90009

10. Dr. E.C. Whipple — 1
Code SS-1
NASA Headquarters
Washington, DC 20546

11. Mr. N. J. Stevens — 1
M2/2165
TRW Space and Technology Group
One Space Park
Redondo Beach, CA 90278

12. Dr. A. R. Fredrickson — 1
Air Force Geophysical Laboratory/PHP
Hanscom AFB, MA 07131

13. Dr. I. Katz — 1
S-Cubed
P.O. Box 1620
La Jolla, CA 92038-1620

14. Dr. M. Mandell — 1
S-Cubed
P.O. Box 1620
La Jolla, CA 92038-1620

15. Dr. V. Davis — 1
S-Cubed
P.O. Box 1620
La Jolla, CA 92038-1620

16. Mr. Gracen Joiner — 1
Code 1114SP
Office of Naval Research
800 N. Quincy St.
Arlington, VA 22217

17. Dr. A. Johnstone — 1
Mullard Space Science Laboratory
University College London
Holmbury St. Mary
Dorking
Surrey RH5 6NT
England

18. Dr. A.J. Coates — 1
Mullard Space Science Laboratory
University College London
Holmbury St. Mary
Dorking
Surrey RH5 6NT
England

19. Dr. G. L. Wrenn — 1
Space Department
Royal Aerospace Establishment
Farnborough,
Hants,
England

20. Dr. Eamonn Daly — 1
ESTEC/WMA
P.O. Box 299
2200 AG Noordwijk
The Netherlands

21. Dr. David Rodgers — 1
ESTEC/WMA
P.O. Box 299
2200 AG Noordwijk
The Netherlands

22. Commander — 1
Naval Space Command
Attn: Code N155
Dahlgren, VA 22448

23. United States Space Command — 1
Attn: Technical Library
Peterson AFB, CO 80914

24. Captain M.P. Scardera — 1
2 SCS/DOAN Stop 82
Falcon AFB, CO 80912-5000

25. LtCol W.L. Shelton — 1
2 SCS/DOAN
Falcon AFB, CO 80912-5000

26. Director — 1
Navy Space Systems Division (OP-943)
Washington, DC 20350-2000

27. Department Chairman, Code 61 — 1
Department of Physics
Naval Postgraduate School
Monterey, CA 93943-5000

28. Major Yan C. WONG — 1
15813 N. 39th Place
Phoenix, AZ 85032